Modelling of Cellular Survival using Monte Carlo Damage Simulation Algorithm

Anestis Dimitris

Master Thesis
MSc. Medical Physics

Department of Medicine
National and Kapodistrian University of Athens

Abstract

This study focuses on the calculation of cellular survival of mammalian cells after irradiation. Double strand breaks are considered the most lethal damage to be induced on a cell. The NHEJ repair pathway is the predominant repair mechanism of DSBs for cells at G1/S phase on cell cycle. A mechanistic model was used to quantify cellular survival as well as other important radiobiological parameters, i.e. RBE, α/β ratio and OER.

The model consists of two input parameters, the average number of primary particles which caused DSBs and the average number of DSBs yield, obtained with MCDS and six fitting parameters that describe biological characteristics of the irradiated cells during the repair process.

Following the estimation of these parameters, the model is applied on further experimental results concerning V79 cells after proton and ^{12}C irradiation. The capability of the model to simulate cellular survival and RBE is partly sufficient, while the impact of molecular oxygen on damage induction is hardly indistinguishable.

Σκοπός της παρούσας εργασίας είναι ο υπολογισμός του ποσοστού επιβίωσης θηλαστικών κυττάρων έπειτα από ακτινοβόληση. Οι βλάβες διπλής έλικας θεωρούνται ως οι πιο θανατηφόρες βλάβες που μπορεί να υποστεί ένα κύτταρο. Ο μηχανισμός $NHEJ$ είναι ο επικρατέστερος μηχανισμός επιδιόρθωσης τέτοιου είδους βλαβών όταν το κύτταρο βρίσκεται στη φάση $G1/S$ του κυτταρικού κύκλου.

Για την ποσοτικοποίηση της κυτταρικής επιβίωσης χρησιμοποιήθηκε ένα μηχανιστικό μοντέλο. Επιπλέον, υπολογίστηκαν σημαντικά ραδιοβιολογικά μεγέθη όπως $RBE, OER, \alpha/\beta ratio$. Το μοντέλο χρησιμοποιεί δύο παραμέτρους οι οποίες υπολογίζονται μέσω του $MCDS$, τη μέση τιμή βλαβών DSB που έχουν σχηματισθεί και τη μέση τιμή του αριθμού των σωματιδίων που προκάλεσαν βλάβη DSB, καθώς και έξι παραμέτρους οι οποίες περιγράφουν βιολογικά χαρακτηριστικά του κυττάρου τα οποία σχετίζονται με τον μηχανισμό επιδιόρθωσης $NHEJ$.

Τον υπολογισμό αυτών παραμέτρων ακολουθεί η εφαρμογή του μοντέλου σε πειραματικά δεδομένα διαφόρων δημοσιεύσεων που περιλαμβάνουν μετρήσεις κυτταρικής επιβίωσης κυττάρων $V79$ έπειτα από ακτινοβόληση με πρωτόνια και ιόντων άνθρακα. Τα μοντελοποιήμενα μεγέθη συγκρίνονται με τα αντίστοιχα πειραματικά. Όπως αποδεικνύεται η επιβίωση των κυττάρων, το RBE και οι όροι α,β προσομοιώνονται μερικώς, ενώ το μοντέλο αποτυγχάνει να αποδόσει την επίδραση του κυτταρικού οξυγόνου.

Supervisor: Professor Georgakilas Alexandros ,NTUA ,SEMFE

I would like to thank PhD candidate Spyridon A Kalospyros for his valuable advice.

Contents

Chapter 1

Theory

1.1 Dose

Radiation dose is the energy (Joules) absorbed per unit mass of tissue and has the (S.I.) units of gray (1 Gy=1 J/kg) [7].

1.2 Linear Transfer Energy

LET is defined as the average energy deposited per unit length of track of radiation and is expressed in keV/μm. It describes the rate of energy deposition of ionizing radiation that transverses through a material. LET is not constant along the length of the track; this is due to the fact that charged particles gradually slow down as they lose part of their Kinetic Energy after each interaction. This results in the emergence of a peak in energy deposition at the end of the track, the Bragg peak. LET is an indicator of radiation quality as it helps to explain some cases of radiation damage disproportionate to the absorbed dose. Generally, charged particles are considered as high-LET radiation while X-rays and γ-rays have low-LET [17].

Typical LET values for commonly used radiations are [10]:
- 250 kVp X rays: 2 keV/μm.
- Cobalt-60 g rays: 0.3 keV/μm.
- 3 MeV X rays: 0.3 keV/μm.
- 1 MeV electrons: 0.25 keV/μm.
- 14 MeV neutrons: 12 keV/μm.
- Heavy charged particles: 100–200 keV/μm
- 1 keV electrons: 12.3 keV/μm.

· 10 keV electrons: 2.3 keV/μm

1.3 RBE

RBE is defined as:

$$\frac{D_{\gamma-ray}}{D_r}$$

where D_r is the test radiation required to produce a particular radiobological effect, the same effect caused by $D_{\gamma-ray}$; it is quite useful as a means of comparison of the effect of different types of radiation. RBE varies with LET, radiation dose, dose rate and biological system. In general, RBE increases along with LET reaching a peak that varies according to ionizing radiation and cellular system.At this point, radiation at this LET is most likely to produce a DSB from one track as the average separation between ionizing event and DNA diameter coincide[5]. Above this peak, RBE starts to decline. This behaviour is due to energy deposition in excess of that needed. As a result, the number of ionizations increases leading to overkill effects. For low LET radiation, the energy deposition events along the track of the radiation are sparse relative to the dimensions of biomolecules such as DNA, thus radiation may pass through matter without depositing any energy For high LET radiation, the energy loss events are much more dense and a significant amount of energy will be deposited along the parts of the track similar in dimension to biomolecules.[8]

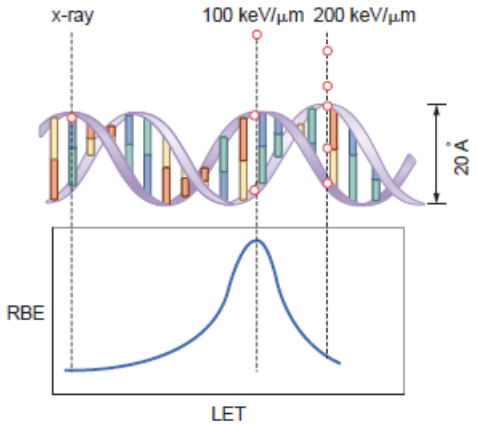

Figure 1.1: RBE reaches a maximum value in terms of the production of DSBs.[21]

1.4 OER

The biological effect of ionizing radiation is affected by the concentration of oxygen in the subcellular environment; the higher the cell oxygenation above anoxia, the larger is the biological imprint of ionizing radiation. As a result, a cell's response to a certain dose differentiates according to molecular oxygen's concentration. The ratio of doses under hypoxic versus normoxic conditions, that produce the same biological effect is called the oxygen enhancement ratio (OER).

$$OER = \frac{Dose\ to\ produce\ a\ given\ effect\ without\ oxygen}{Dose\ to\ produce\ the\ same\ effect\ with\ oxygen}$$

OER is affected by LET; for low LET radiations, biological effect is more intense as oxygen concentration increases, for high LET radiations the oxygen concentration has low impact in cell survival. The maximum value OER can attain is 3.0.

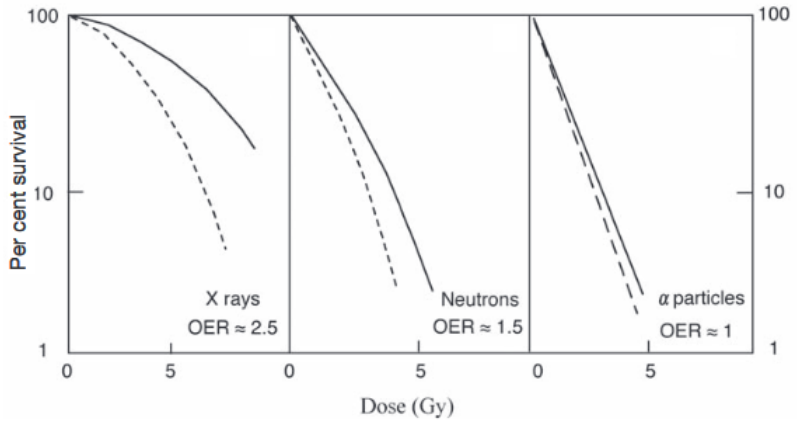

Figure 1.2: Typical cell survival fractions for various LET radiations: dashed curves are for normoxic cell,solid lines for hypoxic cells.[14]

1.5 Types of ionizing radiation

Ionization is a process during which an electron is ejected from its orbit in an atom leaving behind electrically charged particles. A possible outcome is the production of free radicals or the excitation of an atom. These detached particles may subsequently produce significant biological effects in the irradiated material. If the ejected electrons have sufficient energy to directly disrupt the atomic structure of the absorbing medium,

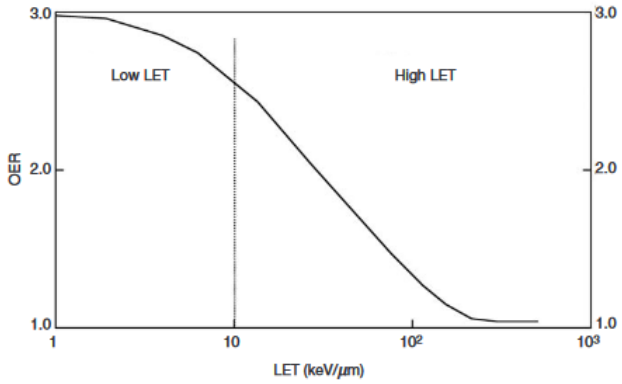

Figure 1.3: LET dependence of OER

this radiation is directly ionizing. On the contrary, if the secondary electrons interact with molecules that would subsequently lead to damage (eg production of OH·), this radiation is indirectly ionizing .

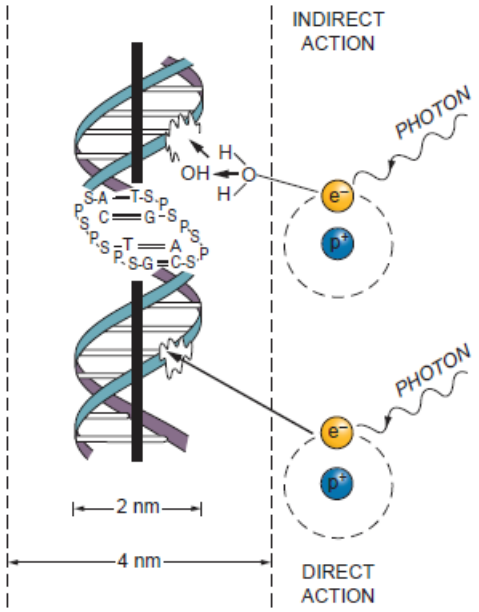

Figure 1.4: Indirect and Direct action of ionizing radiation [22]

1.6 Direct and Indirect effects of radiation

Ionizing radiation can cause chemical reaction that induce damages on biomolecules through direct and indirect effects.

Direct effects are caused by radiation, when energy is directly deposited on a cellular component critical to cell's survival, leading to aberrations in its chemical structure.

Indirect effects are caused by radiation, when energy deposition results in the production of chemical chain reactions which subsequently would impose damages on a biomolecule. One or more bonds of chemical compounds may be broken giving atom or molecules with unpaired electrons; these new compounds are called free radicals.

The indirect action of ionizing radiation is mostly reflected through water radiolysis. The chemical reaction of water radiolysis can be briefly described as:

$$H_2O \rightarrow e_{aq} + OH^\circ + H^\circ + H_2 + H_2O_2$$

The hydroxyl radical are highly reactive with average diffusion distance of about 6 nm [20]. If a biomolecule lies that diffusion range, a new chemical reaction would start leading to the formation of new radicals.

$$RH + OH^\circ \rightarrow R^\circ + H^\circ + H_2O$$

Indirect action of ionizing radiation is the predominant mechanism of damage induction, especially for low LET radiations[11],[3].

The following scheme briefly summarizes the chains of events induced by indirect action of X-rays [3]:

- $Incident\ X-ray\ photon \rightarrow Fast\ electron\ (e^-) \rightarrow ion\ radical \rightarrow Free\ radical \rightarrow Chemical\ changes\ from\ the\ breakage\ of\ bonds \rightarrow Biologic\ effect$

The differences in the time scale involved in these various events are briefly presented below[3]:

- The initial ionization is completed in approximately 10^{-15} seconds.
- The primary radicals produced by the ejection of an electron have a lifetime of 10^{-10} seconds.
- The OH° radical has a lifetime of about 10^{-9} seconds in cells,
- The DNA radicals formed either by direct ionization or by reaction with OH° radicals have a lifetime of approximately 10^{-5} seconds.
- The breakage of chemical bonds and the expression of the biologic effect may take hours, days, months, years, or generations, depending on the consequences involved.

If cell killing is the result, the biologic effect may be expressed hours to days later when the damaged cell attempts to divide.

1.7 DNA Damage

DNA is the principal target for the biological effects of radiation. Aberrations in DNA structure is the primary cause of damages that results in cell death. The most probable DNA lesions are [2]:

- Single Strand Break (SSB)
- Double Strand Break (DSB)
- base damage
- protein-DNA cross links
- protein-protein cross links

The numbers of lesions induced in the DNA of a cell by a dose of 1-2 Gy are approximately: base damages >1000, single strand breaks ∼1000, double strand breaks ∼40.

Double strand breaks are considered the most lethal damage as the repair mechanisms of DNA cannot effectively restore them. This failure leads to chromosomal translocations in DNA helix related to hereditary mutations or carcinogenesis.

1.8 Non-Homologous End Joining (NHEJ) and Homologous Recombination Repair (HRR)

The immediate response of a cell to DNA double strand breaks is the activation of sensitizers that aim to repair the DNA and prevent the cell cycle from proceeding in the cell cycle until the damage is repaired [23].Two are the primary repair pathways, NHEJ and HR. NHEJ operated throughout the cell cycle but is the predominant pathway in G_1/S phase and is an error-prone process. In short, Ku proteins are attached to DNA termini and activate enzymatic components consisting of Pol m and Pol 1 polymerases,DNA-PKc protein kinases and XRCC4 ligase [19]. During NHEJ pathway the NHJEJ complex recognizes and threads onto the DNA double strand break, DNA ends are bridged and stabilized, DNA ends are repairing ligation of the broken ends takes place and finally NHEJ complex dissolves [24]. In competition with NHEJ, acts HR repair pathway, which is an alternative repair mechanism for double strand breaks. This pathway operated throughout S/G_2 phase of the cell cycle and is an error-free process. This repair pathway is completed in sequential steps: nucleolytic resection of blunt ends and binding of NBS/MRE11/rad50 protein complex to the DNA termini, strand exchange facilitated by attachment of rad51/XRCC2 protein, DNA synthesis of the missing nucleotides on the undamaged templates and liga-

tion that creates a complex strand crossover between the damaged and undamaged strands known as a Holliday junction, dissolution of this junction before the repair process is completed [19].

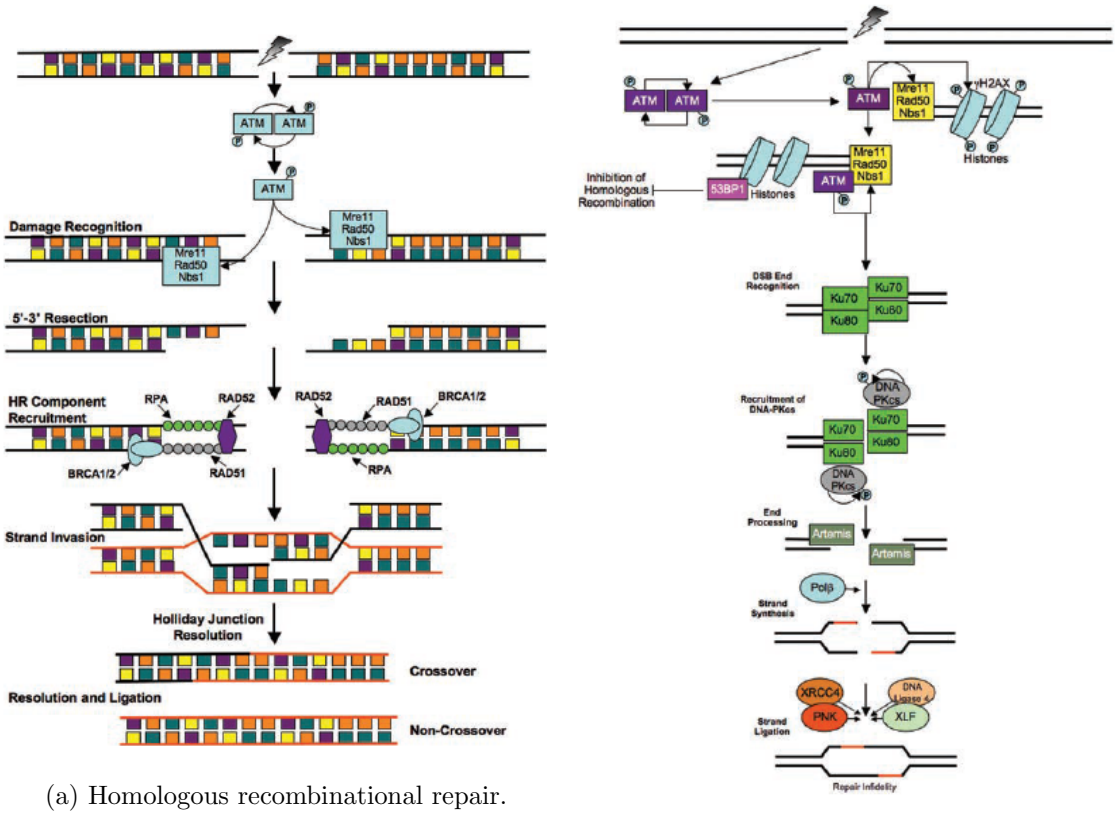

(a) Homologous recombinational repair.

(b) Nonhomologous endjoining.

Figure 1.5: HRR & NHEJ repair mechanisms [16]

1.9 Classification scheme of DNA breaks according to complexity

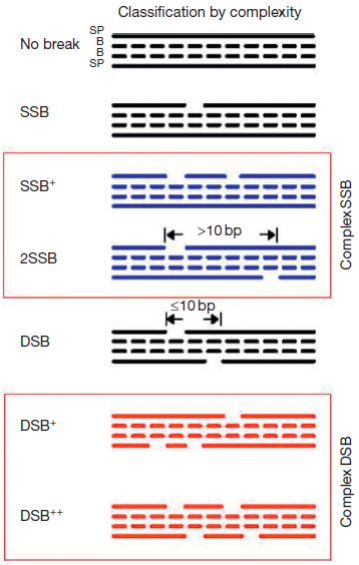

[9]

Figure 1.6: Classification of DNA damage by coplexity withoud consideration of base damage [1]

- No break= segments that were hit but have 'no break' i.e. none of the hits by direct energy deposition or by hydroxyl radicals lead to a strand break,
- SSB= ssb alone
- SSB^{+}= two ssb on the same strand
- 2SSB= two or more ssb on opposite strands but sufficiently separated (>10 bp) as not to be classified as a double strand break
- DSB= two single strand breaks on opposite strands but with a separation < 10 base pairs to constitute a double strand break
- DSB^{+}= a double strand break accompanied by one (or more) additional single strand break within ten base pair separation
- DSB^{++}= more than one double strand break on the segment whether within the ten base pair separation or further apart.

1.10 Linear-Quadratic model

A cell survival curve describes the relationship between the surviving fraction of cells and the absorbed dose. The surviving fraction is graphically represented on a logarithmic scale on the y-axis against dose on a linear scale on the x-axis.

Examples of survival curves for cells irradiated by high LET and low LET ionizing radiation beams are shown in Fig. 1.7.

The shape of the cell survival curve is related to the type of radiation. Densely ionizing radiations exhibit a cell survival curve that is almost an exponential function of dose, shown by an almost straight line on the log–linear plot. For sparsely ionizing radiation, however, the curves show an initial slope followed by a shoulder region and then become nearly straight at higher doses. Factors that reduce radiosensitivity are: low concentration of oxygen to create a hypoxic state, the addition of chemical radical scavengers, the use of low dose rates or multi-fractionated irradiation, and cells synchronized in the late S phase of the cell cycle.

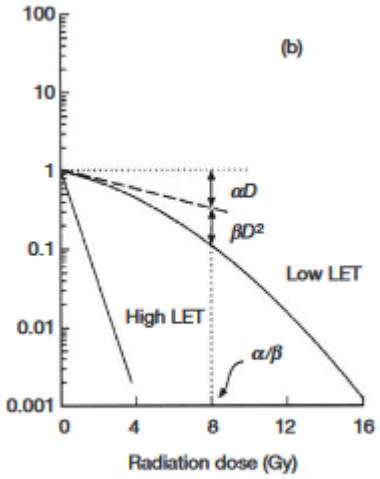

Figure 1.7: Typical cell survival curves for high LET radiation and low LET radiation.The linear quadratic model[13]

The most widely used model to describe cell survival is the linear quadratic model. In this model the fraction of cells surviving a dose D is estimated as:

$$S(D) = e^{-(\alpha D + \beta D^2)}$$

where,

- α, a constant describing the initial slope of the cell survival curve
- β, a smaller constant describing the quadratic component of cell killing.

The ratio α/β gives the dose at which the linear and quadratic components of cell killing are equal. [12]

1.11 Proton and Carbon ion Therapy

Particle therapy is a kind of external beam radiotherapy that uses positively charged particles such as protons and carbon ions. The physical properties of these particles concerning low exit exit doses and an inverse depth dose profile are their main advantages against photons. These lead to a reduced entrance dose and, consequently, a better dose distribution to malignant cells.

Protons used in Radiotherapy

Protons have a certain dose distribution which renders them superior to photons in radiotherapy. Photons distribute most of the energy on a region near the tissue; this short

build-up is followed by an exponential decrease in energy deposition. On the contrary, energy deposition in protons increases alongside with penetration depth until a peak near the end of proton beam range, the Bragg peak [25]. The RBE of protons (1.1) is slightly larger than the RBE of photons (1.0), which means that they are more effective than megavoltage x-rays. Furthermore, the OER for protons is indistinguishable from that for x-rays, namely about 2.5 to 3. Compared to photons used in radiotherapy, for the same dose to the target volume, protons deliver a lower absorbed dose to normal tissues than high-energy x-rays do. Also, malignant cells are exposed to higher radiation dose than normal tissues. Finally, there is little difference in the radiobiological properties of protons used for therapy and high-energy X-rays such as RBE and OER [26].

Carbon ions in Radiotherapy

The physical properties of carbon ions are similar. to those of protons. A view of the dose distribution shows a sharp fall off after the Bragg peak and a distal tail of dose beyond this peak. The radiobiological properties of carbon ions make them applicable to radiotherapy. Dose delivery occurs through ionization events whose density increases along penetration depth until Bragg peak. As LET increases mean ionization density becomes comparable to the DNA helix diameter. Hence, a single particle is capable of inducing a lethal damage to DNA with a single hit.

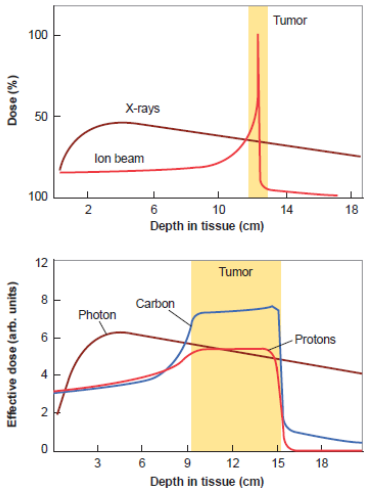

Figure 1.8: Effective dose for protons and Carbon ions compared to X-rays

In figure 1.8, it is distinguishable that both ion beams have a sharp Bragg-peak at the end of the range.However,a realistic tumour can enclose such Bragg-peak.

1.12 References

1. Brahme, A. (2014). Comprehensive biomedical physics. Newnes, pp. 79
2. Dance, D. R., Christofides, S., Maidment, A. D. A., McLean, I. D., & Ng, K. H. (2014). Diagnostic radiology physics: A handbook for teachers and students. Endorsed by: American Association of Physicists in Medicine, Asia-Oceania Federation of Organizations for Medical Physics, European Federation of Organisations for Medical Physics. International Atomic Energy Agency (IAEA): IAEA, pp. 502
3. Hall, E. J., & Giaccia, A. J. (2006). Radiobiology for the Radiologist (Vol. 6), pp. 10
4. Hall, E. J., & Giaccia, A. J. (2006). Radiobiology for the Radiologist (Vol. 6), pp. 104
5. Hall, E. J., & Giaccia, A. J. (2006). Radiobiology for the Radiologist (Vol. 6),pp. 108
6. IAEA, I. (2010). Radiation biology: a handbook for teachers and students. Vienna, Austria: IAEA, pp. 20
7. IAEA, I. (2010). Radiation biology: a handbook for teachers and students. Vienna, Austria: IAEA, pp. 21
8. IAEA, I. (2010). Radiation biology: a handbook for teachers and students. Vienna, Austria: IAEA, pp. 30
9. NIKJOO, P. O'NEILL, DT GOODHEAD and M. TERRISSOL, H. (1997). Computational modelling of low-energy electron-induced DNA damage by early physical and chemical events. International journal of radiation biology, 71(5), 467-483.
10. Podgorsak, E. B. (2005). Radiation oncology physics. Vienna: International Atomic Energy Agency, pp. 486-487
11. Podgorsak, E. B. (2005). Radiation oncology physics. Vienna: International Atomic Energy Agency, pp. 488
12. Podgorsak, E. B. (2005). Radiation oncology physics. Vienna: International Atomic Energy Agency,pp. 492-493
13. Podgorsak, E. B. (2005). Radiation oncology physics. Vienna: International Atomic Energy Agency, pp. 494
14. Podgorsak, E. B. (2005). Radiation oncology physics. Vienna: International Atomic Energy Agency, pp. 499
15. Schulz-Ertner, D., & Tsujii, H. (2007). Particle radiation therapy using proton and heavier ion beams. Journal of clinical oncology, 25(8), 953-964.
16. Hall, E. J., & Giaccia, A. J. (2006). Radiobiology for the Radiologist (Vol. 6),pp. 20-21

17. IAEA, I. (2010). Radiation biology: a handbook for teachers and students. Vienna, Austria: IAEA,pp 20, Hall, E. J., & Giaccia, A. J. (2006). Radiobiology for the Radiologist (Vol. 6),pp. 104
18. Hall, E. J., & Giaccia, A. J. (2006). Radiobiology for the Radiologist (Vol. 6),pp. 108
19. IAEA, I. (2010). Radiation biology: a handbook for teachers and students. Vienna, Austria: IAEA,pp. 26
20. Roots, R., & Okada, S. (1975). Estimation of life times and diffusion distances of radicals involved in X-ray-induced DNA strand breaks or killing of mammalian cells. Radiation research, 64(2), 306-320.
21. Hall, E. J., & Giaccia, A. J. (2006). Radiobiology for the Radiologist (Vol. 6), pp. 109
22. Hall, E. J., & Giaccia, A. J. (2006). Radiobiology for the Radiologist (Vol. 6), pp. 9
23. Hall, E. J., & Giaccia, A. J. (2006). Radiobiology for the Radiologist (Vol. 6),pp. 19
24. Davis, A. J., & Chen, D. J. (2013). DNA double strand break repair via non-homologous end-joining. Translational cancer research, 2(3), 130.
25. Paganetti, H., & Bortfeld, T. (2005). Proton beam radiotherapy-The state of the art. New Technologies in Radiation Oncology (Medical Radiology Series). 2005
26. Hall, E. J., & Giaccia, A. J. (2006). Radiobiology for the Radiologist (Vol. 6),pp 422
27. Rosenblatt, E., Meghzifene, A., Belyakov, O., & Abdel-Wahab, M. (2016). Relevance of particle therapy to developing countries. International Journal of Radiation Oncology Biology Physics, 95(1), 25-29.

Chapter 2

Materials and Methods

2.1 Monte Carlo Damage Simulation Algorithm

The Monte Carlo Damage Simulation (MCDS) algorithm is a quasi - phenomenological concept used to simulate DNA damage yields induced by various types of ionizing radiation, i.e monoenergetic electrons, protons, α-particles and heavy ions with atomic numbers up to Z = 26 with kinetic energies on the order of GeV. Interaction of photons with matter is simulated indirectly through the spectrum of secondary charged particles produced inside the target.The quantities calculated by MCDS are:

- percentage of cluster yields by complexity according to the classification scheme introduced in the previous chapter.
- average number of clusters per cell
- Number of clusters per cell per track
- Cluster Length (in base pair)
- Density of lesions forming a cluster
- Cluster composition

Regarding the spectrum of energy used for the particles involved in MCDS, the minimum allowed kinetic energy depends on the particle type are illustrated in table 2.1:

Moreover, MCDS is capable of simulating the effects of oxygen on the induction of DNA lesions as well as the contribution of free radicals to the diminutions in the total amount of strand breaks and base damages due to the scavenger's presence. Finally, it should be highlighted that MCDS simulates the so called "initial" levels of DNA damage induced and not the processing or repair [4].

Minimum Allowed Kinetic Energy (KE) and Related Properties of Selected Ions in Water as Reported by the MCDS

Particle type	Kinetic energy		$S - S_{rad}$ (keV/μm)	CSDA range (μm)	$\bar{z}_F$ (Gy)	
	MeV	MeV/u			MCDS	Eq. (6)
e^-	2.56×10^{-5}	-	21.13	2×10^{-3}	$<10^{-11}$	0.17
^{1}H	6.47×10^{-3}	6.47×10^{-3}	34.2	0.28	$<10^{-4}$	0.29
$^{3}He^{2+}$	0.222	7.39×10^{-2}	186	2.03	0.06	1.53
$^{4}He^{2+}$	0.294	7.35×10^{-2}	186	2.70	0.14	1.53
$^{12}C^{6+}$	14.8	1.23	612	21.13	5.32	5.08
$^{14}N^{7+}$	24.7	1.76	663	30.42	5.68	5.49
$^{16}O^{8+}$	38.1	2.38	711	42.03	6.01	5.86
$^{20}Ne^{10+}$	78.4	3.92	792	73.14	6.60	6.50
$^{56}Fe^{26+}$	1750	31.3	1148	963.7	9.35	9.34

Figure 2.1: Minimum allowed KE for particles simulated in MCDS and various microdosimetric quantities[3].

The simulation of DNA damage requires the specification of four adjustable parameters [2]:

1. Number of strand breaks Gy^{-1} $cell^{-1}$, σ_{Sb}.
2. Number of base damages Gy^{-1} $cell^{-1}$, σ_{Bd}. The yield of base damages may conveniently be specified in terms of the base damage to strand break ratio, i.e. $f \equiv \frac{\sigma_{Bb}}{\sigma_{Sb}}$.
3. DNA segment length in base pairs (bp) Gy^{-1} $cell^{-1}$, nseg. This DNA segment length is an ad hoc parameter and should not be considered equivalent to the DNA content of a specific chromosome or cell.
4. Minimum length of undamaged DNA (bp) between neighboring elementary damages such that these elementary damages are said to belong to two different lesions, N_{min}.

MCDS algorithm consists of two major steps [2]:

1. random distribution of the expected number of lesions produced in a cell by a specified amount of radiation in a DNA segment (n_{seg})
2. subdivision of the distribution of elementary damages in the segment into lesions. The grouping of lesions into clusters is determined by the N_{min} parameter.

Distribution of lesions in the DNA segment [2]:

1. Compute the parameters for a specific absorbed dose, D (Gy). The segment length cell^{-1} is N_{seg}= $gn_{seg}D$. The total number of strand breaks cell^{-1} is Σ_{Sb}= $g\sigma_{Sb}D$. Here g is a dimensionless scale factor that can be used to adjust the absolute yield of DNA lesions to better mimic experimental observations for specific cell types. In case cell-specific information is unknown, g should be set to unity. The number of base damages cell^{-1} can be calculated from the number of strand breaks cell^{-1}, i.e. σ_{Bd}= f σ_{Sb}.
2. Select a nucleotide pair at random from the DNA segment; i.e., select a uniformly distributed integer in the range [1, N_{seg}].
3. Select a DNA strand (1 or 2) at random. If the selected nucleotide is not already damaged, record the strand break at the location. Otherwise, go to step 2.
4. Set $\Sigma_{Sb} = \Sigma_{Sb}$-1. If $\Sigma_{Sb} > 0$, go to step 2.
5. Repeat steps 2 through 4 for base damages.

The second major step in the damage simulation algorithm is the grouping of lesions into clusters. This grouping procedure identifies a subset of lesions in the DNA segment that can be classified as a unity. DNA clusters arise as a result of energy depositions along radiation tracks in small, of the order of 1–4 nm, isolated regions of DNA that are separated from each other by long segments of undamaged DNA [5]. In MCDS, the N_{min} parameter works as a partition that determines the maximum distance between two consecutive lesions that belong to the same cluster. A modification of N_{min} has direct impact on the clustering of lesions. In case two lesions are separated by at least N_{min} base pairs, they are treated as different clusters. A cluster contains the lesions separated by less than N_{min} base pairs. Moreover, the proposed definition of a cluster guarantees that any lesion in a cluster is within N_{min} bp of another lesion.

Grouping lesions into clusters [1],[2]:

1. Start at one end of the DNA segment and locate the first lesion on either or both strands. Set the start of the cluster to the location of the lesion(s).
2. Starting with the base pair following the last identified lesion, move along the DNA segment in the same direction and count the number of undamaged base pairs present before the next lesion is encountered. If the end of the DNA segment is reached before encountering another lesion, set the end of the cluster to the location of the last detected lesion and quit.
3. If the number of undamaged base pairs is $\geqslant N_{min}$, set the end position of the cluster to the location of the upstream lesion. Then, set the start position of the next cluster to the location of the downstream lesion.

4. Go to step 2.

After all lesions in the DNA segment have been grouped into clusters, the classification scheme of Nikjoo et. al.[9] is applied to categorize the clusters according to the spatial distribution of the constituent lesions. A DSB cluster contains at least one strand break on each DNA strand within 10 bp. All clusters that contain at least one strand break but are not classified as DSBs are marked as SSBs. The remaining clusters are classified as 'base damage'.

Estimation of parameters for the MCDS algorithm

As mentioned above four adjustable parameters are required: f, n_{seg}, N_{min}, σ_{Sb}. The following paragraph is a brief presentation of the method used to calculate these parameters. Semenko et.al.[1] contains a fully detailed presentation of the methodology followed for the estimation of the inputs.

The estimation of the parameters mentioned is based on the interpolated damage yields derived from track-structure simulations (thick line in figure 1). The two sets of track-structure simulations are well approximated by :

$$f(x) = u + \frac{u - w}{x + w}x \tag{2.1}$$

where x≡ $(Z/\beta_{eff})^2$. The thick line in figure 2.2 depicts the damage yield predicted by equation (1) with u = 1134, v = 291, w = 1615 for SSBs and u = 48.9, v = 164.5, w = 759 for DSBs.

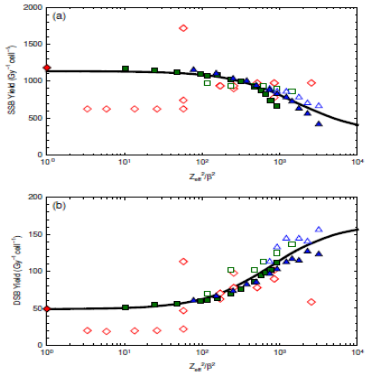

Figure 2.2: Dependence of SSB (a) and DSB (b) yields predicted by detailed Monte Carlo calculations of Nikjoo et. al. [12],[13],[14],[15] and Friedland et. al. [10],[11]

The optimization of the following criterion results in the estimation of the MCDS parameters

$$C = \sum_{n=1}^{2} \frac{(O_i - E_i)^2}{E_i} \tag{2.2}$$

Here, O_i is the yield of the ith type of damage obtained with the MCDS algorithm and E_i is the interpolated yield for the ith type of damage; indices 1 and 2 refer to SSBs and DSBs. Optimization of criterion C is repeated with the interpolated SSB and DSB yields corresponding to a number of $(Z/\beta_{eff})^2$ values ranging between 1 and 10.000 and the best-fit values of MCDS parameters (n_{seg}, σ_{Sb} and N_{min}) are obtained as a function of $(Z/\beta_{eff})^2$. The inputs for the MCDS algorithm calculated by the procedure above are:

σ=1300 Gy^{-1} $cell^{-1}$
f=3
$n_{seg}(x) = 149200 - \frac{123600x}{x+267}$ $bp\ Gy^{-1} cell^{-1}$
$N_{min} = 9\ bp$

2.1.1 Specification of radiation quality

Effective charge: The effective charge of a positive or negative ion is calculated according to 'Barkas' formula [8] as

$$Z_{eff} = Z[1 - exp(125 \cdot \beta \cdot Z^{-2/3})] \tag{2.3}$$

and β is given by

$$\beta = \sqrt{1 - \frac{1}{(1 + T/m_0c^2)^2}} \tag{2.4}$$

where T is the kinetic energy of the charged particle, and m_0c^2 is the rest mass energy of the charged particle. The ratio of the square of the effective charge and the square of the particle's speed relative to the speed of light in a vacuum, $(Z_{eff}/\beta)^2$, is used in the MCDS as the preferred indicator of radiation quality. For ions with $Z > 2$, simulation parameters are assumed the same for all ions with the same $(Z_{eff}/\beta)^2$.

Quantities reported by MCDS [3]

- charged-particle stopping power in liquid water . For monoenergetic electrons, protons and a particles with kinetic energies greater than 10 keV, stopping powers in liquid water are based on an empirical fit to data from the National Institute of Standards and Technology STAR database (http://www.nist.gov/physlab/data/star/). For electrons with kinetic energies below 10 keV, collisional stopping powers in liquid water are based on an empirical fit to data from the IXS-D3 model of Emfietzoglou and Nikjoo [6]. For $Z > 2$, charged particle stopping power in water is equated

to the stopping power of an a particle with the same $(Z_{eff}/\beta)^2$. For photons, the MCDS computes a fluence-averaged stopping power from the spectrum of secondary electrons produced after the interaction with the target cell.

- frequency-mean specific energy ($\overline{z_F} = 0.3059\overline{\Delta E}/\rho d^3$) where d is the diameter of the cell nucleus of the target and $\overline{\Delta E}$ is the average energy deposited (in keV) by ions passing through a target with density q (g cm^{-3}) and diameter d (in μm).
- lineal energy $\overline{y_F}$.
- the absorbed dose per unit fluence $D/\Phi = \pi d^2 \overline{z_F}/4$.
- the average path length R traveled by a charged particle as it slows down, as calculated using the continuous-slowing-down approximation (i.e., the CSDA range).
- The average energy $\overline{\Delta E}$ (keV) deposited in the target is the integral of the chord length l times the stopping power weighted by the relative number of particles traveling distance l, i.e

$$\overline{\Delta E} = \int_0^{min(R,d)} dl \cdot l f(l)[S(l) - S_{rad}(l)] \tag{2.5}$$

where f(l) is the distribution of chord lengths, f(l)dl is the fraction of the particles traveling distance [l, l+dl] with collisional (electronic) and nuclear stopping power S(l)– $S_{rad}(l)$. The integration range from 0 to min(R, d) ensures that the energy deposited in the target does not exceed the particle's kinetic energy. For a spherical body exposed to a uniform isotropic fluence of particles traveling in straight lines, f(l)=$\frac{2l}{d^2}$ (64), and Eq. (5) becomes:

$$\overline{\Delta E} = \int_0^{min(R,d)} dl \cdot l^2[S(i) - S_{rad}(l)] \tag{2.6}$$

When S– S_{rad} (in keV/μm) is constant while the particle passes through a target and the CSDA range of the particle of interest is large compare to the diameter of cell nuclues, eq. (6) is approximated as :

$$\overline{\Delta E} = \frac{2d}{3}[S - S_{rad}] \tag{2.7}$$

2.1.2 Simulation of the effects of free radical scavengers

The numbers of strand breaks, σ_{Sb}, and base damages, σ_{Bb}, decrease in inverse proportion to the scavenger concentration, [S]. The simulation of the effects of free radical scavengers, such as dimethyl sulfoxide (DMSO) is achieved by multiplying σ_{Sb} with the following dimensionless function:

- $[S]$= concentration of scavenger
- ϕ[S]= the fraction of strand breaks and base damages that are not scavengeable.
- K[S]= the concentration at which function h is reduced to its half-value, i.e. $(1 + \phi)/2$. The number of base damages distributed within the DNA segment is determined using $\sigma_{Bb} = h([S]) \cdot f \cdot \sigma_{Sb}$, where f= 3.

Normal cellular environment corresponds to zero scavenger concentration (normal cellular enviroment) eq. h→1. For very large scavenger concentrations, eq. h→ ϕ .In that case the numbers of strand breaks and base damages distributed within the DNA segment are $\phi\sigma_{Sb}$ and $\phi f\sigma_{Sb}$, respectively.

2.1.3 Effects of Radiation Quality and Oxygen on Clustered DNA Lesions and Cell Death

Simulation of the effects of chemical repair and oxygen fixation:

In a normoxic environment, the initial DNA radicals formed through direct or indirect damage mechanisms may interact with O_2, endogenous thiols or other cellular constituents. The reduction of DNA radicals by thiols has been termed chemical repair. Oxygen fixation, a process which postulates that radical-induced DNA damage can be permanently 'fixed' by molecular oxygen [15], rendering DNA damage irreparable, acts alongside chemical repair.

To simulate the effects of oxygen on the formation of individual and clustered DNA lesions within the MCDS, a three-step algorithm is used [3]:

Step 1. Simulate the number and location within the DNA of individual and clustered DNA radicals. The radical and lesion clustering effects arising from the structure of individual particle tracks are preserved.
Step 2. Determine probability p_R an initial DNA radical formed by ionizing radiation undergoes chemical repair. The fraction of the initial DNA radicals removed through the chemical repair process is determined using the formula:

$$p_R(x, [O_2]) = 1 - \frac{[O_2] + K}{[O_2] + M(x) \cdot K}$$

- $[O_2]$ = %O_2 concentration at the time of irradiation,
- (1 – 1/M) = the maximum fraction of DNA radicals removed through chemical repair under fully anoxic conditions $[O_2]$=0
- K = %O_2 at which half of the maximum is removed, and
- x =$(Z_{eff}/\beta)^2$

As $(Z_{eff}/\beta)^2$ increases the effectiveness of chemical repair decreases. This is due to factors such as radical clustering or other chemical modifications to the DNA This effect is modeled using the empirical formula M(x):

$$M(x) = M_0 - \frac{M_0 - 1}{1 + (q/x)^r}$$

M_0, q and r are adjustable parameters that capture essential physiochemical factors and processes that hamper the chemical repair process in vitro or in vivo.

- M_0 is the maximum fraction of the DNA radicals that can be removed through chemical repair, and the term involving the ratio
- q/x is a correction for changes in the effectiveness of chemical repair with radiation quality. For low- LET radiations, q/x is large, oxygen fixation is minimized and chemical repair is maximized.

For q/x$\rightarrow \infty$, M(x) approaches the asymptotic value M_0. As particle LET increases, q/x decreases, M(x)$\rightarrow$1, and oxygen fixation is maximized.

Step 3. Remove fraction p_R(x,[O_2]) of the DNA radicals created in step 1. It is assumed that all of the initial DNA radicals created in step 1 are equally likely to be removed through the chemical repair process. This hypothesis conjectures that all of the initial DNA radicals forming a putative cluster are equally accessible to O_2 and to DNA radical scavengers in the cellular environment as well as the interaction kinetics among DNA radicals, scavengers and O_2 is assumed not to saturate.

HRF for individual and clustered DNA lesions [3]:

Hypoxia Ratio Factor (HRF) is the ratio of the absorbed dose required to produce biological effect E under maximally hypoxic conditions to the absorbed dose required to produce the same effect E under normoxic conditions.Although the definition is identical to OER there is a qualitative difference; HRF is an indicator of radiation sensitivity of cells under reduced oxygen that quantifies the effect of oxygen concentration on DNA damage. The HRF for DSB induction, HRF_{dsb}, can be expressed as a ratio of doses or as a ratio of DSB yields :

$$HRF_{dsb}\ ([O_2]) = \frac{D([O_2])}{D_N}$$

The form of HRF is presumed upon the linear relation between the induction of DNA damage and absorbed dose up to at least a few hundreds of Gy of low- or high-LET radiation regardless of oxygen concentration. Term D_N describes the absorbed dose required to cause $\sigma_N\ DSB\ (Gy^{-1}Gbp^{-1})$ in cells irradiated under normoxic conditions, and D([O_2]) the absorbed dose required to cause $\sigma([O_2])\ DSB\ (Gy^{-1}Gbp^{-1})$ in cells irradiated under oxygen concentration [O_2].

In MCDS HRF_{ssb} and HRF_{dsb} are approximated as

$$HRF_{ssb}\ ([O_2]) \backsimeq \frac{1}{1 - p_r(x, [O_2])} \tag{2.8}$$

$$HRF_{dsb}\ ([O_2]) \backsimeq (\frac{1}{1 - p_r(x, [O_2])})^2 \tag{2.9}$$

Eguation (8) is derived on basis that SSBs must be composed of at least one strand break. Therefore the chemical repair (p_R) of a DNA radical with the potential to form a strand break will produce a corresponding reduction in the measured SSB yield In a similar way, DSBs are composed of a minimum of two strand breaks on opposed DNA strands, and the chemical repair of the DNA radical to either of the strand breaks forming a DSB will reduce the number of measured DSBs [3]. Hence, this behaviour is described by equation (9).

The oxygen effect parameters selected as optimal are:
M_0 =1.740, K= 0.3372% O_2, q= 946.1, r = 2.150.

2.2 A mechanistic model of cellular survival

Methods

A mechanistic model of cellular survival following radiation induced DNA double-strand breaks proposed by Wang et. al [17] was used.The aim of this mechanistic model is to predict the relationship between radiation induced DSBs in the nucleus of the cell and probability of cell survival. The proposed model makes use of two input parameters calculated with assistance from MCDS and four fitting parameters that biologically describe a cell.The two input parameters are:
(1) the average number of primary particles that cause DSB, n_p
(2) the average number DSBs yielded by each primary particle that causes DSBs,λ_p.
The remaining four parameters will be described in detail below.

Parameters λ_p, $\mathbf{n}_p$

The average number of radiation induced DSBs per cell is given by:

$$N = Y * D \tag{2.10}$$

,where Y ≡ DSB yield per Cell per Gy, D ≡ radiation dose to the nucleus.

The number of primary particles passing through the nucleus,n,is calculated by:

$$n = \frac{\pi R^2 * D * \rho}{LET * 1.602 * 10^{-19}} * 10^{-18} \tag{2.11}$$

,where R ≡ radius of cell nucleus (μm), ρ ≡ density of cell nucleus (g/cm^3).

Consequently,the DSB yield per cell per primary particle, λ, can be derived by:

$$\lambda = \frac{N}{n} \tag{2.12}$$

Given that the number of DSBs yielded by a primary particle follows Poisson distribution, the probability of a primary particle passing through a cell nucleus without causing DSB equals to:

$$P(X = 0) = \frac{\lambda^0}{0!} e^{-\lambda} \tag{2.13}$$

These primary particles have no role in cell death. Thus, the probability of a primary particle passing through a cell nucleus causing DSB equals to 1-exp(-λ). Thus,

$$n_p = n(1 - e^{-\lambda}) = \frac{YD}{\lambda}(1 - e^{-\lambda}) \tag{2.14}$$

$$\lambda_p = \frac{\lambda}{1 - e^{-\lambda}} \tag{2.15}$$

Quantities Y and λ can calculated directly with MCDS. Then, n_p and λ_p can be calculated with equation (5) (6) respectively.
As mentioned in the previous section, the two most important mechanisms of DSB repair are homologous recombination repair (HRR) pathway and the nonhomologous end-joining (NHEJ) pathway. HRR is an error-free process thus the probability that a DSB is repaired correctly is high and not taken into account.On the contrary, NHEJ is error-prone so it is considered as the mechanism which contributed the most to cell death.
For a DSB to be repaired correctly by NHEJ pathway,each DSB should:

1. not be joined with a DSB end from a DSB induced by a different primary particle.By assuming that primary particles distribute randomly, the probability this condition is met equals to:

$$P_{interaction} = \frac{1 - e^{-\eta(\lambda_p) n_p}}{\eta(\lambda_p) n_p} \tag{2.16}$$

where $\eta(\lambda_p)$ n_p is the average probability of a DSB end being joined with a DSB end from a DSB induced by a different primary particle.The relationship between $\eta(\lambda_p)$ and λ_p is:

$$\begin{cases} \eta(\lambda_p) = \eta_{\lambda_p \to \infty} - \dfrac{\eta_{\lambda_p \to \infty} - \eta_{\lambda_p \to 1}}{\lambda_p} \\ lim_{\eta_{\lambda_p \to 1}} \eta(\lambda_p) = \eta_{\lambda_p \to 1} \\ lim_{\eta_{\lambda_p \to \infty}} \eta(\lambda_p) = \eta_{\lambda_p \to \infty} \end{cases} \tag{2.17}$$

2. not be joined with a DSB end from a different DSB induced by the same primary particle By assuming that DSBs generated by a primary particle are randomly distributed on its track:

$$P_{track} = \frac{1 - e^{-\xi\lambda_p}}{\xi\lambda_p} \tag{2.18}$$

   where $\xi\lambda_p$ is the average probability of a DSB end being joined with a DSB end from a different DSB induced by the same primary particle.
3. be joined with the other end from the same DSB correctly. The average probability is assumed to be μ_x.
   The probability of a DSB being correctly repaired is:

$$P_{correct} = \mu_x P_{interaction} P_{track} = \mu_x (\frac{1 - e^{-\eta(\lambda_p)n_p}}{\eta(\lambda_p)n_p})(\frac{1 - e^{-\xi\lambda_p}}{\xi\lambda_p}) \tag{2.19}$$

Taking into consideration the over kill effect, not all DSBs induced by radiation have contribution to cell death. The probability of a DSB relating to cell death in given by:

$$P_{contribution} = \frac{1 - e^{-\zeta\lambda_p}}{\zeta\lambda_p} \tag{2.20}$$

,where $\zeta\lambda_p$ is the average probability of a DSB contributing to cell death.

Therefore, the average number of lethal events equals to:

$$N_{death} = \mu_y N * P_{contribution} * (1 - P_{correct}) \tag{2.21}$$

Cell survival according to LQ model can be derived by:

$$-lnS = N_{death} \tag{2.22}$$

$$S = exp(-\mu_y N * (\frac{1 - e^{-\zeta\lambda_p}}{\zeta\lambda_p}) * (1 - \mu_x (\frac{1 - e^{-\eta(\lambda_p)n_p}}{\eta(\lambda_p)n_p})(\frac{1 - e^{-\xi\lambda_p}}{\xi\lambda_p}))) \tag{2.23}$$

By applying Taylor expansion to $P_{interaction}$:

$$P_{interaction} == \frac{1 - e^{-\eta(\lambda_p)n_p}}{\eta(\lambda_p)n_p} = 1 - \frac{1}{2}\eta(\lambda_p)n_p + O(\eta(\lambda_p)n_p) \tag{2.24}$$

When n_p is small enough,$O(\eta(\lambda_p)n_p) \to 0$.

If we substitute equations (15),(11) and (10) to equation (13) we come up with equation:

$$-lnS = \alpha D + \beta D^2 \tag{2.25}$$

where,

$$\alpha = Y * (\frac{1 - e^{-\zeta\lambda_p}}{\zeta\lambda_p}) * (1 - \mu_x(\frac{1 - e^{-\xi\lambda_p}}{\xi\lambda_p})) * \mu_y \tag{2.26}$$

$$\beta = \frac{1}{2}\eta(\lambda_p)\frac{Y}{\lambda_p} * Y * (\frac{1 - e^{-\zeta\lambda_p}}{\zeta\lambda_p}) * (\frac{1 - e^{-\xi\lambda_p}}{\xi\lambda_p}) * \mu_x\mu_y \tag{2.27}$$

- α term of the LQ model refers to the DSBs induced by a single primary particle and their interactions concerning over-kill effect and DNA clustered damage effect.
- β term refers to the DSBs induced by different primary particles.

Estimation of parameters μ_x, μ_y, ζ, ξ, $\eta_{\lambda_p \to 1}$, $\eta_{\lambda_p \to \infty}$ The experimental data of cell survival curves were extracted from Furusawa et.al [4]. The data consist of experimental estimations of $\alpha(\text{Gy}^{-1})$,D_{10}(Gy) for V79 mammalian cells (5.6 Gbp) after irradiation by ^{3}He, ^{12}C, ^{20}Ne ions at various energies under normoxic conditions. Also, a cell survival for 200 kVp X-rays is included. D_{10}(Gy) is the dose at 10% of the survival rate. Therefore, β parameters can be derived by:

$$\beta = -\frac{ln(0.1) + \alpha D_{10}}{D_{10}^2} \tag{2.28}$$

In some experimental measurements β parameters correspond to negative values. These values are neglected because they have no radiobiological content.

A typical mammalian cell's nucleus diameter is about 10μ and its cell diameter is about 20μm. MCDS input parameters for the simulation were:

SIMCON: nocs=10000 seed=987654321
CELL: DNA=5.6 ndia=10 cdia=20 WEM=0
EVO2: pO2=21 m0=1.740 k=0.3372 q=946.1 r=2.150
RADX: PAR=3He or 12C or 20Ne MeV/A=... AD=1
DMSO: CONC=0 FNSD=0.52 CHMX=0.21
MCDS: fbl=0.25

The parameter fitting for the estimation of the six parameters is completed in three steps:

1. Firstly,μ_x, μ_y, ζ and ξ were obtained with the experimental data of α values as well as the calculated n_p and λ_p. Consequently the modelled data of α values could be obtained with equation (2.26).
2. Then, with the μ_x, μ_y, ζ and ξ obtained above as well as the experimental data of cell survival in X-ray, $\eta_{\lambda_p \to 1}$ was obtained with equation (2.23).
3. Finally with the mu_x, mu_y, ζ and ξ and $\eta_{\lambda_p \to 1}$ obtained above, $\eta_{\lambda_p \to \infty}$ was obtained with the experimental data of β values. Consequently, the modelled data of β values could be obtained with equation (2.27).

The evaluation of the parameters above was implemented on MATLAB using non-linear regression.

2.3 References

1. Semenenko, V. A., & Stewart, R. D. (2006). Fast Monte Carlo simulation of DNA damage formed by electrons and light ions. Physics in Medicine & Biology, 51(7), 1693.
2. Semenenko, V. A., & Stewart, R. D. (2004). A fast Monte Carlo algorithm to simulate the spectrum of DNA damages formed by ionizing radiation. Radiation research, 161(4), 451-457.
3. Stewart, R. D., Yu, V. K., Georgakilas, A. G., Koumenis, C., Park, J. H., & Carlson, D. J. (2011). Effects of radiation quality and oxygen on clustered DNA lesions and cell death. Radiation research, 176(5), 587-602.
4. Chatzipapas, K. P., Papadimitroulas, P., Emfietzoglou, D., Kalospyros, S. A., Hada, M., Georgakilas, A. G., & Kagadis, G. C. (2020). Ionizing Radiation and Complex DNA Damage: Quantifying the Radiobiological Damage Using Monte Carlo Simulations. Cancers, 12(4), 799.
5. Brenner, D. J., & Ward, J. F. (1992). Constraints on energy deposition and target size of multiply damaged sites associated with DNA double-strand breaks. International journal of radiation biology, 61(6), 737-748.
6. Emfietzoglou, D., & Nikjoo, H. (2007). Accurate electron inelastic cross sections and stopping powers for liquid water over the 0.1-10 keV range based on an improved dielectric description of the Bethe surface. Radiation Research, 167(1), 110-120.
7. Roots, R., & Okada, S. (1975). Estimation of life times and diffusion distances of radicals involved in X-ray-induced DNA strand breaks or killing of mammalian cells. Radiation research, 64(2), 306-320.

8. Barkas, W. H. (1973). Nuclear research emulsions,pp 371
9. NIKJOO, P. O'NEILL, DT GOODHEAD and M. TERRISSOL, H. (1997). Computational modelling of low-energy electron-induced DNA damage by early physical and chemical events. International journal of radiation biology, 71(5), 467-483.
10. Friedland, W., Jacob, P., Bernhardt, P., Paretzke, H. G., & Dingfelder, M. (2003). Simulation of DNA damage after proton irradiation. Radiation Research, 159(3), 401-410.
11. Friedland, W., Dingfelder, M., Jacob, P., & Paretzke, H. G. (2005). Calculated DNA double-strand break and fragmentation yields after irradiation with He ions. Radiation Physics and Chemistry, 72(2-3), 279-286.
12. NIKJOO, P. O'NEILL, DT GOODHEAD and M. TERRISSOL, H. (1997). Computational modelling of low-energy electron-induced DNA damage by early physical and chemical events. International journal of radiation biology, 71(5), 467-483.
13. Nikjoo, H., E. Bolton, C., Watanabe, R., Terrissol, M., O'Neill, P., & T. Goodhead, D. (2002). Modelling of DNA damage induced by energetic electrons (100 eV to 100 keV). Radiation protection dosimetry, 99(1-4), 77-80.
14. Nikjoo, H., O'Neill, P., Terrissol, M., & Goodhead, D. T. (1999). Quantitative modelling of DNA damage using Monte Carlo track structure method. Radiation and environmental biophysics, 38(1), 31-38.
15. Nikjoo, H., O'Neill, P., Terrissol, M., & Goodhead, D. T. (1994). Modelling of radiation-induced DNA damage: the early physical and chemical event. International journal of radiation biology, 66(5), 453-457.
16. Grimes, D. R., & Partridge, M. (2015). A mechanistic investigation of the oxygen fixation hypothesis and oxygen enhancement ratio. Biomedical physics & engineering express, 1(4), 045209.

    Wang, W., Li, C., Qiu, R., Chen, Y., Wu, Z., Zhang, H., & Li, J. (2018). Modelling of cellular survival following radiation-induced DNA double-strand breaks. Scientific reports, 8(1), 1-12.

Chapter 3

Results

3.1 Comparison between experimental and modelled reuslts

The biological parameters μ_x, μ_y, ζ, ξ, $\eta_{\lambda_p \to 1}$, $\eta_{\lambda_p \to \infty}$ were calculated according to the fitting method proposed in the previous chapter ,using experimental measurements of Furusawa's dataset [4] :

	Estimation	SE
μ_x	0.95242	0.07329
μ_y	0.03924	0.04686
ζ	0.038777	0.03443
ξ	0.033555	0.03591
$\eta_{\lambda_p \to 1}$	0.00088101	$7.51\ 10^{-6}$
$\eta_{\lambda_p \to \infty}$	0.0049831	0.0007

Figures (3.1 a) and (3.2 b) depict the two categories of α and β terms. Comparison of α terms shows a satisfactory agreement with R^2= 0.8515. On the contrary, β terms have low R^2= 0.095. This may attributed to two factors. For LET $<$ 100 keV/μm experimental β values are widely scattered. For LET $>$ 100 keV/μm β values are very small compared to α. Therefore, contribution of β to cell survival is so lean that it is hardly detectable in experimental measurements.

Afterwards,survival dose at 10%, RBE at 5%, 10%, 50% are illustrated in figure (3.2). Comparison shows a good agreement between modelled and experimental data with R^2= 0.7939, R^2= 0.8035, R^2= 0.8345, R^2= 0.8675 respectively. Despite the agreement, there is room for improvement as for LET$<$ 30 keV/μm in figure (3) modelled data behave quite differently than experimental data. The same behaviour regulates the RBE values but to a lesser extent.

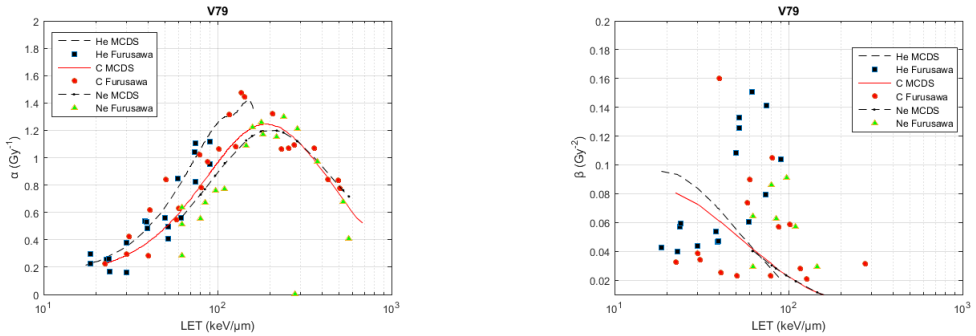

(a) (b)

Figure 3.1: Comparison between experimental and modelled α, β terms

A qualitative view on figure (3.2) shows that RBE for ^{12}C has a peak at LET$\sim$189 keV/μm. This result is close to experimental measurements which show that RBE peak appears at $\sim$175 [7]. Also, experimental data prove that RBE peak of V79 cells after ^{3}He irradiation appears at 100 keV/μm [2], while on modelled data the peak appears at 149 keV/μm.

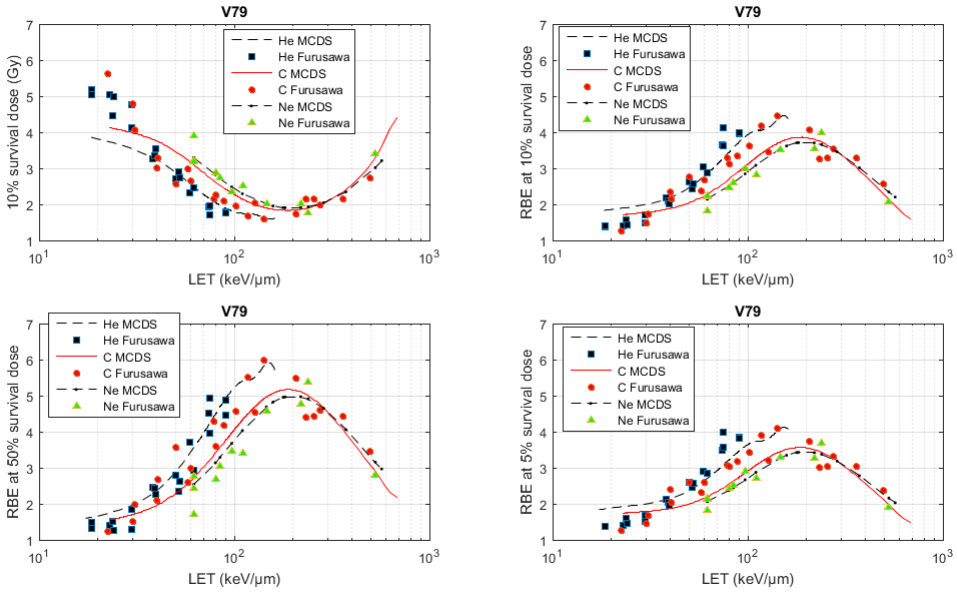

Figure 3.2

Next, cell survival curves for V79 cells irradiated by ^{12}C ions at various LET values

is calculated as shown in figure (3.3). It is observed β term's contribution to cell survival decreases as well as the slope of cell survival declines in inverse proportion to LET until 206 keV/μm. For 360 keV/μm and 502 keV/μm the slope inclines. This behaviour is expected as in figure (1) α reaches a peak at 200 keV/μm. The R^2 of comparison is $\sim$0.9 for all survival curves.

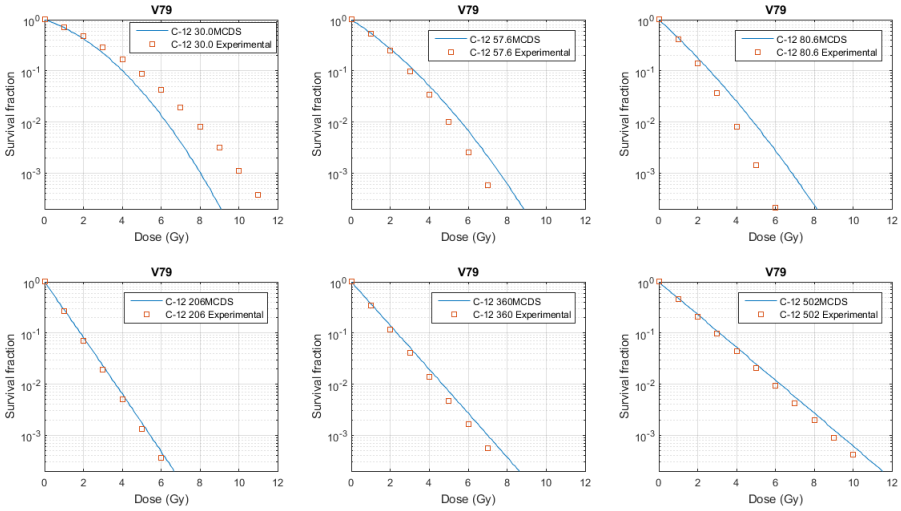

Figure 3.3: Survival Curves of V79 cells after ^{12}C ions irradiation.

Finally, figure (3.4) shows the α/β ratio as derived by modelled and experimental data. This ratio is regarded as an indicator or cellular capacity in the LQ model. It can be shown that it increases alongside with LET. This may be attributed to two factors :

- α terms increase with LET due to the cluster DNA damage effect
- the number of primary particles delivering dose to the nucleus decreases with LET so that the interaction of DSBs induced by different particles are very unlikely to interact.

For LET $>$ 100 keV/μm ,α β values differ above 2 orders of magnitude; this reinforces the statement that β values' contribution to cell survival is so small, that it is hard to be measured in some experimental data.

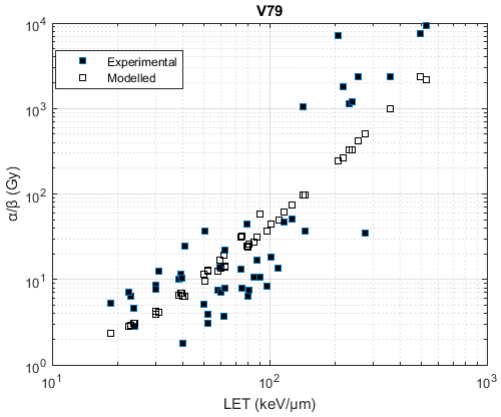

Figure 3.4

The mechanistic model is further applied on experimental data of V79 cells other than the ones included in Furusawa's dataset.

Firstly, α and β terms of V79 cells after proton irradiation are derived. As shown in figure (3.5) for 5<LET<30 keV/μm there is big divergence between experimental and modelled data, which tends to reduce as LET increases further than 30 keV/μm.

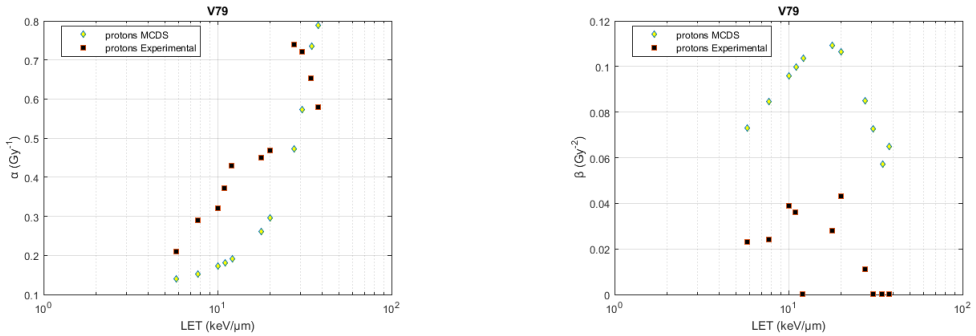

(a) (b)

Figure 3.5: Comparison between experimental and modelled values of α, β for protons. Experimental values are extracted by Perris et al.[5],Folklard et al.[3],Belli et al.[1]

Furthermore, the RBE of protons is illustrated in figure (3.6). A peak at 50 keV/μm for modelled protons. However, it is known that the peak is expected at 30.5 keV/μm (Belli et. al[1]). This difference may be attributed to the estimated values of the biological parameters of the model; a bigger dataset would probably lead to a better estimation as well as more accurate simulations. The comparison of Dose Survival at 10% ,RBE at 10%, RBE at 5%, RBE at 50 % gives R^2= 0.9607, R^2= 0.9649, R^2= 0.9556, R^2= 0.9825

respectively.

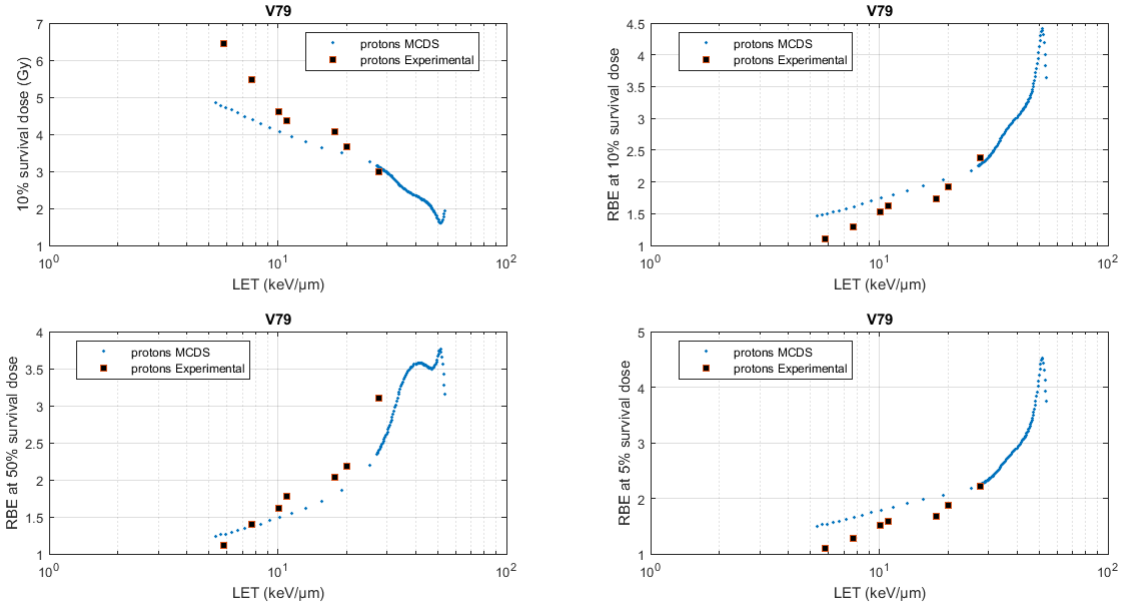

Figure 3.6

The survival curves of cells after proton irradiation under normoxic conditions and hypoxic conditions are, also, calculated in figure (3.7), and compared to experimental data from Prise et al[6] in figure (3.8). It is observed that the mechanistic model fails to reproduce the experimental data. The modelled data are strongly affected to β term of $S=e^{-(\alpha D^2+\beta D^2)}$ compared to experimental data. As a result OER is underestimated. Moreover, OER in modelled curved is stable at ~ 1.2, although it is expected that OER reduces inversely to LET.

The mechanistic model is capable of producing different survival curves according to oxygen concentration; the radiosensitivity is in inverse proportion to oxygen concentration. However, the modelled OER values are not aligned with theoretical values of OER. It would be expected that low LET radiations would have OER$\sim$ 2.

Finally, the survival curves of V79 cells irradiated with protons at different LET are illustrated at figure (3.9). A comparison between experimental and modelled data gives $R^2 \sim 0.9$. However, a qualitatively comparison shows that there is huge divergence between the measurements. The modelled survival curves the cell survival decreases as LET increases. After 30.5 keV/μm the slope of cell survival should increase but the modelled data do not behave accordingly.

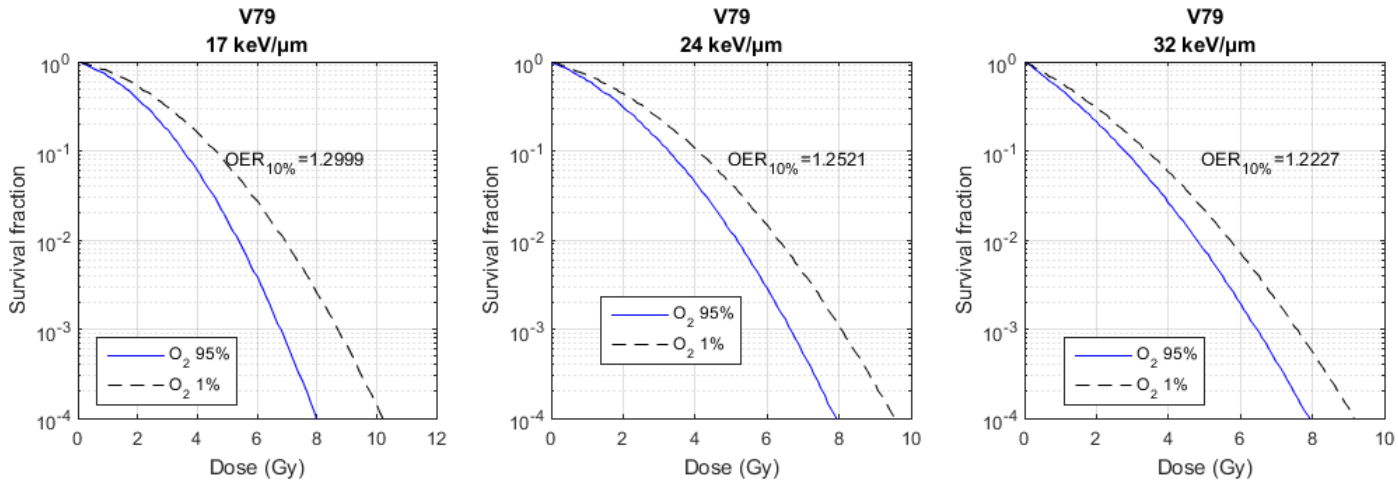

Figure 3.7: Survival curves under normoxic and hypoxic conditions for protons, OER at 10% of survival,modelled curves

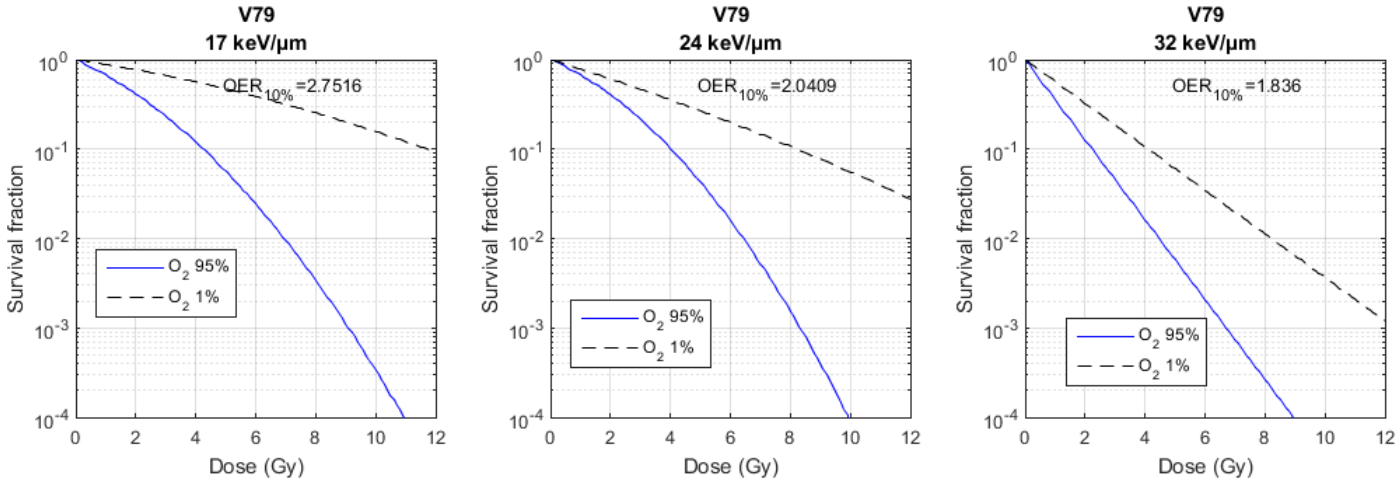

Figure 3.8: Survival curves under normoxic and hypoxic conditions for protons, OER at 10% of survival,experimental curves from Prise et al.[6]

In addition, the mechanistic model was used to reproduce experimental results of cells after ^{12}C irradiation included in various experiments.

At first, the cell survival of carbon ions of different LET is calculated. The results are depicted in figure (3.10).

It is observed that cell survival decreases as LET increases from 13.7 keV/μm to 153.5 keV/μm and increases again for 482.7 keV/μm. This result is not consistent with the

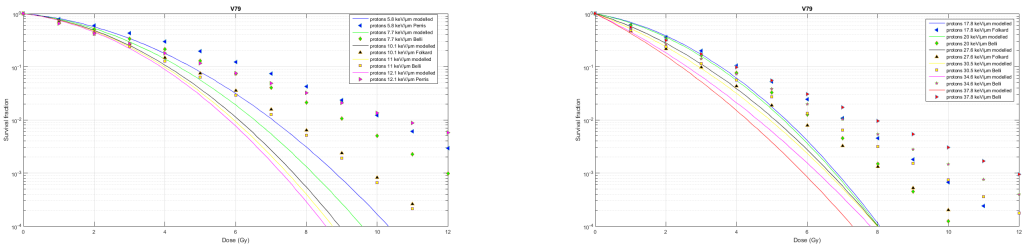

(a) (b)

Figure 3.9: Comparison between experimental and modelled values of cellular survival for protons. Experimental values are extracted by Perris et al.[5],Folklard et al.[3],Belli et al.[1]

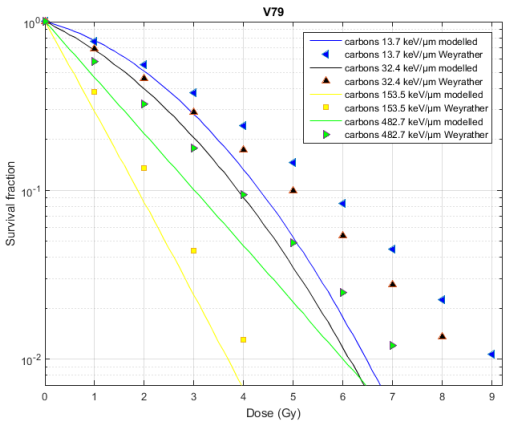

Figure 3.10: Survival curves after carbon irradiation, data from Weyrather et.al[7]

theoretical statement that cell survival reduces as LET increases. A possible explanation of this behaviour is attributed to the fact that the peak of α term for carbon ions for V79 cells is observed approximately at 175 keV/μm. Consequently, the contribution of α to $SF = e^{-(\alpha D+\beta D^2)}$ gradually weakens for LET $>$ 175 keV/μm, therefore the slope of SF declines. The R^2 coefficient that results from the comparison between modelled and experimental measurements is approximately 0.9.

Finally, the survival curves at certain LET values for aerobic and hypoxic conditions are calculated. The results are shown in figure (3.11). OER reduces in inverse proportion to LET, as it would be expected according to figure (1.2) in Chapter "Theory". For LET$>$ 100 keV/μm OER tends toward unity; for 10$<$LET$<$40 keV/μm OER is approximately 2. Survival curves of low LET radiation in figure (3.11) have $OER_{10\%}$ $\sim$1.3, thus the experimental and modelled results are divergent. As LET increases OER$\rightarrow$1; for LET=153.5

keV/μm and LET=482 keV/μm is practically 1.

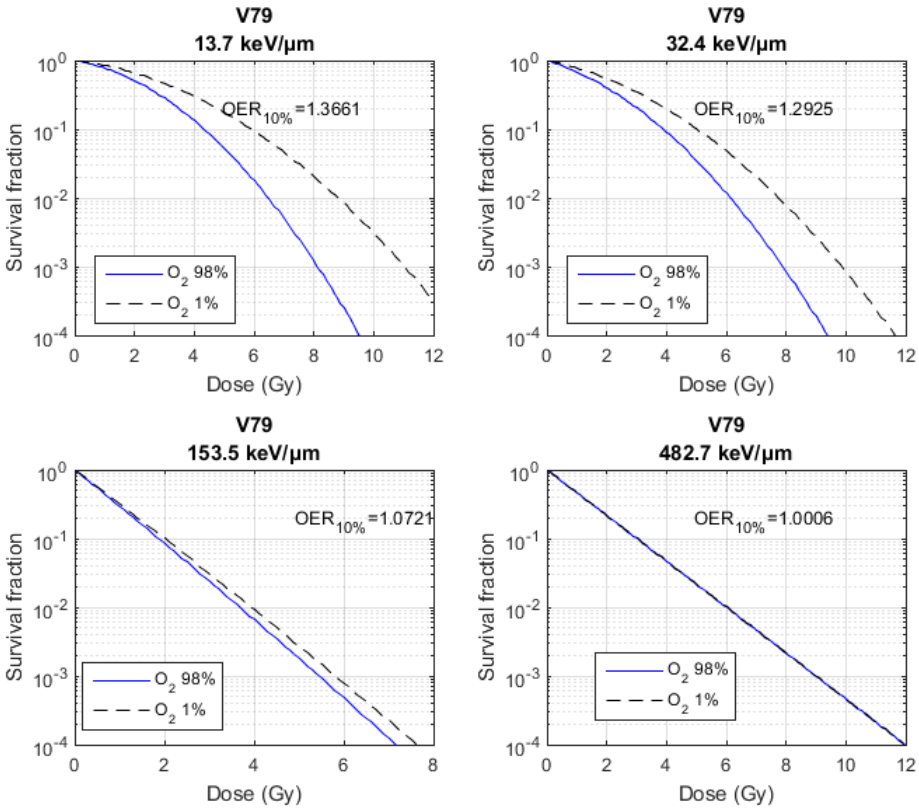

Figure 3.11: OER at 10% after ^{12}C irradiation

3.2 Discussion

Double strand breaks are assumed as the initial lesions in the DNA that could result in a lethal damage The NHEJ repair mechanism, an error prone process, is the predominant repair mechanism of DSBs for cells at G1/S phase of the cell cycle. A mechanistic model was used to quantify cellular survival of cells following radiation induced DSBs. The model contains two parameters two input parameters, the average number of primary particles which caused DSBs and the average number of DSBs yield, as well as six fitting parameters that describe biological characteristics of a cell. The two input parameters are directly obtained with MCDS. The estimation of the biological parameters is accomplished by fitting the model to experimental data concerning carbon, helium and neon ions.

After the calculation of the parameters, a comparison between α and β terms, RBE, cellular survival, Dose at 10% and α/β ratio between experimental and modelled data takes place. The comparison shows good agreement.

The model is further applied n measurements of proton and carbon ions, other than the ones used for parameter fitting. In case of protons, t is observed that the model fails to reproduce the experimental data. Terms β have low agreement,while terms α converge for LET$>$ 20 $keV/mu\ m$. The modelled RBE peak shows up at 50 keV/μm instead of 30.5 keV/μm. Also, OER at various LET is calculated. The model gives insufficient results.

For carbon ions, the model gives survival curves similar to the experimental ones. However, OER cannot be reproduced. Thus, the model gives inadequate calculations of the impact cellular oxygen has on irradiated cells.

In conclusion, further improvements on the model should be made so that the mechanistic model could give prominence to crucial role of cellular oxygen and provide us with better estimations concerning α and β terms. A dataset that includes measurements of extra particles may improve that estimation of fitting parameters, and, consequently, of the rest radiobiological quantities.

3.3 Appendix

Furusawa et.al.[4]			MCDS	Experimental Values		Simulation Values			
Ion	LET	MeV/A	MeV/A	$\alpha(Gy^{-}1)$	$\beta(Gy^{-}2)$	$\alpha(Gy^{-}1)$	$\delta\alpha$	$\beta(Gy^{-}2)$	$\delta\beta$
^{3}He	18.6	10.1	9.66	0.225	0.043	0.225	0.0004	0.096	2.0E-07
	23	7.73	7.4	0.255	0.040	0.271	0.0005	0.093	2.0E-07
	23.8	7.39	7.1	0.261	0.057	0.279	0.0005	0.092	2.0E-07
	24	7.3	7.03	0.168	0.059	0.281	0.0005	0.092	2.0E-07
	29.9	5.5	5.34	0.376	0.044	0.352	0.0006	0.084	2.0E-07
	38.1	4.07	3.93	0.534	0.054	0.465	0.0007	0.072	1.0E-07
	39.2	3.92	3.79	0.529	0.047	0.481	0.0007	0.070	1.0E-07
	39.4	3.9	3.77	0.486	0.047	0.483	0.0007	0.070	1.0E-07
	50	2.83	2.77	0.561	0.108	0.642	0.0009	0.056	8.0E-08
	51.9	2.72	2.644	0.405	0.133	0.672	0.0009	0.053	7.0E-08
	52.3	2.7	2.616	0.496	0.126	0.677	0.0009	0.053	7.0E-08
	58.9	2.33	2.24	0.848	0.060	0.777	0.0010	0.046	6.0E-08
	61.9	2.16	2.1	0.56	0.151	0.820	0.0011	0.043	5.0E-08
	73.9	1.65	1.654	1.04	0.079	0.988	0.0012	0.032	4.0E-08
	74.6	1.62	1.632	1.105	0.141	1.000	0.0012	0.031	4.0E-08
	90.8	1.27	1.241	1.117	0.104	1.181	0.0013	0.020	2.0E-08
^{12}C	22.5	126	122.08	0.227	0.032	0.225	0.0004	0.081	2.0E-07
	30	82.3	82.6	0.295	0.038	0.288	0.0005	0.073	2.0E-07
	31	78.6	79.2	0.427	0.034	0.296	0.0005	0.072	2.0E-07
	40.1	55.6	56.8	0.283	0.160	0.385	0.0006	0.061	1.0E-07
	40.6	54.8	55.89	0.619	0.025	0.389	0.0006	0.061	1.0E-07
	50.3	41.7	42.62	0.841	0.023	0.490	0.0008	0.051	1.0E-07
	57.6	35.4	35.97	0.549	0.074	0.568	0.0008	0.045	8.0E-08
	60	33.5	34.18	0.631	0.090	0.593	0.0009	0.043	7.0E-08
	78.5	25.2	24.48	1.021	0.023	0.780	0.0011	0.032	5.0E-08
	80.6	24.5	23.7	0.781	0.105	0.799	0.0011	0.031	4.0E-08
	88	21.9	21.25	0.971	0.057	0.865	0.0011	0.027	4.0E-08
	102	18.1	17.7	1.066	0.059	0.978	0.0013	0.022	3.0E-08
	117	14.9	14.92	1.315	0.028	1.072	0.0013	0.017	2.0E-08
	127	13.9	13.47	1.08	0.021	1.123	0.0013	0.015	2.0E-08
	142	12.4	11.707	1.446	0.001	1.180	0.0014	0.012	1.0E-08
	206	7.6	7.258	1.323	0.000	1.240	0.0013	0.005	5.0E-09
	232	6.37	6.197	1.064	0.001	1.216	0.0013	0.004	3.0E-09
	255	5.64	5.45	1.07	0.000	1.182	0.0012	0.003	2.0E-09
	276	5.09	4.884	1.091	0.032	1.144	0.0012	0.002	2.0E-09
	360	3.42	3.309	1.07	0.000	0.981	0.0010	0.001	8.0E-10
	493	1.98	1.966	0.837	0.000	0.750	0.0007	0.000	2.0E-10
^{20}Ne	62.1	130	123.12	0.511	0.064	0.566	0.0009	0.040	7.0E-08
	62.2	129	122.85	0.634	0.029	0.567	0.0009	0.040	7.0E-08
	80	84.2	87.25	0.555	0.086	0.730	0.0010	0.030	5.0E-08
	84.6	78.6	81.03	0.672	0.063	0.770	0.0011	0.028	4.0E-08

96.9	68.1	67.88	0.761	0.091	0.869	0.0012	0.023	3.0E-08
110	57.5	57.64	0.774	0.057	0.960	0.0013	0.019	3.0E-08
146	38.4	40.28	1.087	0.029	1.126	0.0014	0.012	1.0E-08
219	24.7	24.216	1.15	0.001	1.198	0.0013	0.005	4.0E-09
239	21.7	21.689	1.299	0.001	1.185	0.0013	0.004	4.0E-09
528	7.71	7.546	0.675	0.000	0.763	0.0007	0.000	3.0E-10

protons	Folkard et.al[3]	Belli et.al.[1]		Perris et. al.[5]				
	MCDS	LET	Experimental		Simulations			
MeV/A	MeV/A	keV/μm	α(Gy^{-1})	β(Gy^{-2})	α(Gy^{-1})	$\delta\alpha$(Gy^{-1})	β(Gy^{-2})	$\delta\beta$(Gy^{-2})
7.4	7.305	5.8	0.21	0.023	0.1403	3.0E-04	0.0729	3.0E-07
3	2.906	12.1	0.43	0	0.1911	8.0E-04	0.1036	1.0E-07
3.66	3.66	10.1	0.32	0.039	0.1720	8.0E-04	0.0960	1.0E-07
1.83	1.762	17.8	0.45	0.028	0.2605	8.0E-04	0.1094	1.0E-07
1.07	0.9659	27.6	0.74	0.011	0.4732	8.0E-04	0.0848	1.0E-07
1.41	1.5	20	0.469	0.043	0.2969	8.0E-04	0.1065	1.0E-07
3.2	3.283	11	0.372	0.036	0.1804	8.0E-04	0.0999	1.0E-07
5.01	5.142	7.7	0.289	0.024	0.1534	8.0E-04	0.0845	1.0E-07
0.57	0.6022	37.8	0.58	0	0.7888	8.0E-04	0.0650	1.0E-07
0.64	0.6914	34.6	0.653	0	0.7360	8.0E-04	0.0571	1.0E-07
0.76	0.835	30.5	0.721	0	0.5731	8.0E-04	0.0723	1.0E-07

Weyrather et.al[7]								
	MCDS	LET	Experimental		Simulations			
^{12}C	MeV/A	keV/μm	α(Gy^{-1})	β(Gy^{-2})	α(Gy^{-1})	$\delta\alpha$(Gy^{-1})	β(Gy^{-2})	$\delta\beta$(Gy^{-2})
	258.4	13.7	0.234	0.03	0.171	4.0E-04	0.084	2.0E-07
	186.6	16.8	0.226	0.03	0.190	4.0E-04	0.085	2.0E-07
	74.75	32.4	0.337	0.025	0.316	5.0E-04	0.071	2.0E-07
	10.6093	153.5	0.91	0.044	1.214	1.40E-03	0.010	1.0E-08
	2.0421	482.7	0.533	0.014	0.765	7.0E-04	0.000	3.0E-10

Prise et.al.[6]	LET	MCDS	Experimental		Simulations			
	keV/μm	MeV/A	α_N	β_N(Gy^{-2})	α_N(Gy^{-1})	$\delta\alpha_N$(Gy^{-1})	β_N(Gy^{-2})	$\delta\beta_N$(Gy^{-2})
	17	1.87	0.35	0.045	0.2547	4.0E-04	0.112	2.0E-07
Protons	24	1.175	0.33	0.060	0.3852	6.0E-04	0.099	2.0E-07
	32	0.778	1.03	0.000	0.6437	9.0E-04	0.066	9.0E-08

Prise et.al.[6]	LET	MCDS	Experimental		Simulations			
	keV/μm	MeV/A	α_H(Gy^{-1})	β_H(Gy^{-2})	α_H	$\delta\alpha_H$(Gy^{-1})	β_H(Gy^{-2})	$\delta\beta_H$(Gy^{-2})
	17	1.87	0.116	0.007	0.1370	4.0E-04	0.072	2.0E-07
Protons	24	1.175	0.239	0.005	0.2640	5.0E-04	0.074	2.0E-07

32	0.778	0.561	0.000	0.4837	7.0E-04	0.057	1.0E-07

$$\delta\alpha = \sqrt{(\frac{\partial\alpha}{\partial Y}\delta\alpha)^2 + (\frac{\partial\alpha}{\partial\lambda_p}\delta\lambda_p)^2 + (\frac{\partial\alpha}{\partial\mu_x}\delta\mu_x)^2 + (\frac{\partial\alpha}{\partial\mu_y}\delta\mu_y)^2 + (\frac{\partial\alpha}{\partial\xi}\delta\xi)^2 + (\frac{\partial\alpha}{\partial\zeta}\delta\zeta)^2}$$

$$\delta\beta = \sqrt{(\frac{\partial\beta}{\partial Y}\delta\alpha)^2 + (\frac{\partial\beta}{\partial\lambda_p}\delta\lambda_p)^2 + (\frac{\partial\beta}{\partial\mu_x}\delta\mu_x)^2 + (\frac{\partial\beta}{\partial\mu_y}\delta\mu_y)^2 + (\frac{\partial\beta}{\partial\xi}\delta\xi)^2 + (\frac{\partial\beta}{\partial\zeta}\delta\zeta)^2 + (\frac{\partial\beta}{\partial\eta}\delta\eta)^2}$$

3.4 References

1. Belli, M., Cherubini, R., Finotto, S., Moschini, G., Sapora, O., Simone, G., & Tabocchini, M. A. (1989). RBE-LET relationship for the survival of V79 cells irradiated with low energy protons. International journal of radiation biology, 55(1), 93-104.
2. Barendsen, G. W., Walter, H. M. D., Fowler, J. F., & Bewley, D. K. (1963). Effects of different ionizing radiations on human cells in tissue culture: III. Experiments with cyclotron-accelerated alpha-particles and deuterons. Radiation research, 18(1), 106-119.
3. Folkard, M. "Inactivation of V79 cells by low-energy protons, deuterons and helium-3 ions." International journal of radiation biology 69.6 (1996): 729-738.
4. Furusawa Y, Fukutsu K, Aoki M, et al. Inactivation of aerobic and hypoxic cells from three different cell lines by accelerated (3)He-, (12)C- and (20)Ne-ion beams [published correction appears in Radiat Res. 2012 Jan;177(1):129-31]. Radiat Res. 2000;154(5):485-496.
5. Perris, A., Pialoglou, P., Katsanos, A. A., & Sideris, E. G. (1986). Biological effectiveness of low energy protons. I. Survival of Chinese hamster cells. International Journal of Radiation Biology and Related Studies in Physics, Chemistry and Medicine, 50(6), 1093-1101.
6. Prise, K. M., Folkard, M., Davies, S., & Michael, B. D. (1990). The irradiation of V79 mammalian cells by protons with energies below 2 MeV. Part II. Measurement of oxygen enhancement ratios and DNA damage. International journal of radiation biology, 58(2), 261-277.
7. K. Weyrather, S. Ritter, M. Scholz, G. Kraft, W. "RBE for carbon track-segment irradiation in cell lines of differing repair capacity." International journal of radiation biology 75.11 (1999): 1357-1364.

3.5 MATLAB

The code used for the calculation of biological parameters:

At first,the experimental data should be organized in an excel file as : Ion,Dose Averaged LET,MeV/A,MeV/A in MCDS, Z^2/β^2,α(Gy$^-$1) D10(Gy) β (Gy^{-2})

The data used for fitting are shown in the following table:

Ion	Dose Averaged LET	MeV/A	MeV/A at MCDS	Z/β^2	$\alpha(Gy^-1)$	D_{10}(Gy)	$\beta(Gy^{-2})$
^{3}He	18.6	10.1	9.66	196	0.225	5.17	0.042625589
	18.6	10.1	9.66	196	0.297	5.04	0.031718675
	23	7.73	7.4	255	0.255	5.04	0.040052008
	23.8	7.39	7.1	26	0.261	4.47	0.056850046
	24	7.3	7.03	269	0.168	4.98	0.059109736
	29.9	5.5	5.34	354	0.162	4.76	0.067591673
	29.9	5.5	5.34	354	0.376	4.13	0.043953186
	38.1	4.07	3.93	482	0.534	3.25	0.05368853
	39.2	3.92	3.79	500	0.529	3.36	0.046515828
	39.4	3.9	3.77	504	0.486	3.53	0.047107761
	50	2.83	2.77	692	0.561	2.7	0.108077516
	51.9	2.72	2.644	729	0.405	2.91	0.132737579
	52.3	2.7	2.616	736	0.496	2.74	0.125678658
	58.9	2.33	2.24	864	0.848	2.33	0.060186243

	61.9	2.16	2.1	922	0.56	2.47	0.150696634
	73.9	1.65	1.654	1179	1.04	1.93	0.07930014
	74.6	1.62	1.632	1195	1.105	1.71	0.141252041
	74.6	1.62	1.632	1195	0.822	1.95	0.184006599
	90.8	1.27	1.241	1578	0.956	1.79	0.184558876
	90.8	1.27	1.241	1578	1.117	1.77	0.103895781
^{12}C	22.5	126	122.08	169	0.227	5.63	0.032324142
	30	82.3	82.6	239	0.295	4.8	0.038480256
	31	78.6	79.2	248	0.427	4.07	0.034089858
	40.1	55.6	56.8	337	0.283	3.01	0.160125726
	40.6	54.8	55.89	342	0.619	3.28	0.02530721
	50.3	41.7	42.62	446	0.841	2.56	0.022830977
	57.6	35.4	35.97	520	0.549	2.99	0.073944933
	60	33.5	34.18	544	0.631	2.65	0.089773598
	78.5	25.2	24.48	736	1.021	2.15	0.023241772
	80.6	24.5	23.7	756	0.781	2.26	0.105240248
	88	21.9	21.25	836	0.971	2.11	0.057001211
	102	18.1	17.7	989	1.066	1.95	0.058878394
	117	14.9	14.92	1160	1.315	1.69	0.028092536
	127	13.9	13.47	1280	1.08	2.05	0.021079142
	137	12.9	12.247	1401	1.477	1.56	-0.00063071
	142	12.4	11.707	1460	1.446	1.59	0.00136272
	206	7.6	7.258	2280	1.323	1.74	0.000186647
	232	6.37	6.197	2640	1.064	2.16	0.000931304
	255	5.64	5.45	2980	1.07	2.15	0.000451075
	276	5.09	4.884	3290	1.091	1.995	0.031668166
	360	3.42	3.309	4670	1.07	2.15	0.000451075
	432	2.55	2.474	6060	0.844	2.73	-0.00020595
	493	1.98	1.966	7300	0.837	2.75	0.000110426
	502	1.92	1.9	7500	0.779	2.96	-0.0003715
^{20}Ne	62.1	130	123.12	466	0.511	3.21	0.064272968
	62.1	130	123.12	466	0.286	3.91	0.077467121
	62.2	129	122.85	467	0.634	3.17	0.029138024
	80	84.2	87.25	631	0.555	2.87	0.086165316
	84.6	78.6	81.03	675	0.672	2.73	0.062797715
	96.9	68.1	67.88	793	0.761	2.36	0.090962563
	110	57.5	57.64	922	0.774	2.51	0.057117362
	146	38.4	40.28	1310	1.087	2.01	0.029136678
	158	35.7	36.488	1430	1.225	1.88	-0.00011739
	178	31.1	31.41	1620	1.259	1.83	-0.00041354
	182	30.2	30.54	1660	1.169	1.97	-8.8873E-05
	219	24.7	24.216	2050	1.15	2	0.000646273
	239	21.7	21.689	2260	1.299	1.77	0.001070922
	287	17.5	17.186	2790	1.212	1.9	-5.9531E-05
	373	12.8	12.21	3810	0.968	2.38	-0.00022154

528	7.71	7.546	5820	0.675	3.41	7.18168E-05
569	7.1	6.758	6390	0.409	5.63	-2.6787E-06

The extract algorithm extracts data from the measurements obtained with MCDS. MCDS measurments should be saved in form "Number.txt"

```
function [Tableone,Tabletwo,Tablethree,Tablefour,Tablefive,Tablesix
...,Energies,Dose,ZF,LET,MeVperA]=extract(pathname);
addpath (pathname)
 n = numel(dir([pathname '/*.txt']));
Tableone=zeros(n,11);
Energies=zeros(n,1);
EffectiveCharge=zeros(n,1);
DNA=zeros(n,1);
DMSO=zeros(n,1);
LET=zeros(n,1);
Tabletwo=zeros(n,8);
Tablethree=zeros(n,8);
Tablefour=zeros(n,8);
Tablefive=zeros(n,8);
Tablesix=zeros(n,8);
Oxygen=zeros(n,1);
ZF=zeros(n,1);
for q=1:n
        w=num2str(q);t='.txt';filename=[w t];
        a=table2cell(readtable(filename));
        if size(a,1)==395
            disp('DNA content bigger than nucleus')
            return
        end
         BD= strsplit(cell2mat(a(90)));BD=str2num(cell2mat(BD(1,1)));
        SSB= strsplit(cell2mat(a(91)));SSB=str2num(cell2mat(SSB(1,1)));
        SSBp= strsplit(cell2mat(a(92)));SSBp=str2num(cell2mat(SSBp(1,1)));
        SSB2= strsplit(cell2mat(a(93)));SSB2=str2num(cell2mat(SSB2(1,1)));
        DSB= strsplit(cell2mat(a(94)));DSB=str2num(cell2mat(DSB(1,1)));
        DSBp= strsplit(cell2mat(a(95)));DSBp=str2num(cell2mat(DSBp(1,1)));
        DSBpp= strsplit(cell2mat(a(96)));DSBpp=str2num(cell2mat(DSBpp(1,1)));
        SSBc= strsplit(cell2mat(a(97)));SSBc=str2num(cell2mat(SSBc(1,1)));
        SSBcb= strsplit(cell2mat(a(98)));SSBcb=str2num(cell2mat(SSBcb(1,1)));
        DSBc= strsplit(cell2mat(a(99)));DSBc=str2num(cell2mat(DSBc(1,1)));
        DSBcb= strsplit(cell2mat(a(100)));DSBcb=str2num(cell2mat(DSBcb(1,1)));
        Tableone(q,:)=[BD,SSB,SSBp,SSB2,DSB,DSBp,DSBpp,SSBc,SSBcb,DSBc,DSBcb];
        MeV=strsplit(cell2mat(a(24)));MeV=str2num(cell2mat(MeV(1)));MeVperA(q,1)=MeV;
        E= strsplit(cell2mat(a(44)));E=str2num(cell2mat(E(3)));Energies(q,1)=E;
        dmso= strsplit(cell2mat(a(84)));dmso=str2num(cell2mat(dmso(1)));DMSO(q,1)=dmso;
        ox= strsplit(cell2mat(a(76)));ox=str2num(cell2mat(ox(1)));Oxygen(q,1)=ox;
```

```
        Efc= strsplit(cell2mat(a(45)));Efc=str2num(cell2mat(Efc(2)));
        EffectiveCharge(q,1)=Efc;
        dna=strsplit(cell2mat(a(8)));dna=str2num(cell2mat(dna(1)));DNA(q,1)=dna;
        Let=strsplit(cell2mat(a(46)));Let=str2num(cell2mat(Let(3)));LET(q,1)=Let;
        ad=strsplit(cell2mat(a(7)));ad=str2num(cell2mat(ad(1)));Dose(q,1)=ad;
        zf=strsplit(cell2mat(a(52)));zf=str2num(cell2mat(zf(6)));ZF(q,1)=zf;
        mcl=strsplit(cell2mat(a(15)));mcl=str2num(cell2mat(mcl(3)));
        MeanChordLength(q,1)=mcl;
      %
      %
      % Table2
      % Clusters per cell
       C = strsplit(cell2mat(a(158)));
       for i=2:9
           Tabletwo(q,i-1)=str2num(cell2mat(C(i)));
       end
        % Table3
       C = strsplit(cell2mat(a(219)));
       for i=2:9
       %Clusters per Cell per Track
           Tablethree(q,i-1)=str2num(cell2mat(C(i)));
       end
        % Table4
       C = strsplit(cell2mat(a(276)));
       for i=2:9
       %Cluster length (in base pair)
           Tablefour(q,i-1)=str2num(cell2mat(C(i)));
       end
        % Table5
       C = strsplit(cell2mat(a(333)));
       for i=2:9
       %Density of lesions forming a cluster
           Tablefive(q,i-1)=str2num(cell2mat(C(i)));
       end
        % Table6
       C = strsplit(cell2mat(a(391)));
       for i=2:9
       %Cluster composition (% Sb per Cluster)
           Tablesix(q,i-1)=str2num(cell2mat(C(i)));
       end
end

end
```

The step1 algorithm calculates λ, λ_p, N that are essential inputs to the Wang's model.

```
function [Y,lambda,N,np,lambdap]=step1(Tabletwo,Lambda,Dose)
```

```
Y=Tabletwo(:,1)./Dose./1 ;% 1=1 cell
lambda=Lambda(:,1);
N=Y(:,1).*Dose;
np=N./lambda.*(1-exp(-lambda));
lambdap=lambda./(1-exp(-lambda));
end
```

The fitting for the estimation of biological parameters :

```
%% Load Data
clc;clear;
n=1;
[num,~,~] = xlsread('Excel that contains the experimental data of Furusawa') ;
a=num(:,5);
b=num(:,7);
tLET=num(:,1);
Experimental=table(a,b);
pathName='Folder that contains simulations of MCDS'
[~,Tabletwo,Lambda,~,~,~,Dose,~,LET,~]=extract(pathName);
[Y,~,~,~,lambdap]=step1(Tabletwo,Lambda,Dose);
T=[Experimental.a Y lambdap Experimental.b LET tLET];
B=[];

% Cleaning measurments that contain negative b values
for i=1:size(T,1)
if T(i,end-2)>0
    B=[B;T(i,:)];
end
end
J=[];i=1;
while i <=size(B,1)
    if i==2 || i==6 || i==18 || i==19 || i==43
        i=i+1;
        if i==19
            i=i+1;
        end
    end
    J=[J;B(i,:)];
    i=i+1;
end
T=J;
theoretical_a=T(:,1);
X=[T(:,2) T(:,3)  ];

%% Fitting of a

rng('default') % for reproducibility
```

```
A=@(b,X) X(:,1).* (1-exp(-b(3)*X(:,2))).*(b(3)*X(:,2)).*(1-b(1)*...
(1-exp(-b(4)*X(:,2))).*(b(4)*X(:,2)))*b(2);

%% Run Model
b =  [0.95126;0.04;0.04;0.04];
beta0 = [0.95126;0.04;0.04;0.04];

opts = statset('nlinfit');opts.RobustWgtFun ='bisquare';
mdl1= fitnlm(X,theoretical_a,A,beta0,'Options',opts)
p=mdl1.Coefficients.Estimate;

modelled_a=A(p,X);
clearvars opts

%% Fitting of SF


clearvars Tabletwo Lambda Dose LET lambdap X
[~,Tabletwo,Lambda,~,~,~,~,Dose,~,LET,~]=extract('Folder MCDS measurements2');
[~,~,N,np,lambdap]=step1(Tabletwo,Lambda,Dose);
N=N*7.07; % 7.07 Dose at 10% survival for X-Rays, it is experimental data
np=np*7.07;
X=[N,lambdap,np];
mx=p(1);my=p(2);z=p(3);ksi=p(4);
 SF=@(heta,X) exp(-my.*X(:,1).*(1-exp(-z.*X(:,2))./(z.*X(:,2)).*
 ...(1-mx.*(1-exp(-ksi.*X(:,2)))./
 ...(ksi.*X(:,2)).*(1-exp(-heta.*X(:,3)))./(heta.*X(:,3))));
theoretical_SF=zeros(size(X,1),1);theoretical_SF(:,1)=0.1;

%%
rng('default') % for reproducibility
heta =0.0024053 ;heta0 =0.0008462;

opts = statset('nlinfit');opts.RobustWgtFun ='bisquare';
mdl2= fitnlm(X,theoretical_SF,SF,heta0,'Options',opts)
hetaOne=mdl2.Coefficients.Estimate;

D=7.07*ones(22,1);F=exp(-0.184*D-0.02*D.^2);
plot(SF(hetaOne,X),'d');hold on ;plot(F,'o');hold off
%%
clearvars Experimental  B a b Tabletwo lambdap Dose LET X

%% Fitting of b

theoretical_b=T(:,4);
X=[T(:,2) T(:,3)  ];
```

```
%%
B=@ (heta,X) 0.5*(heta-(heta-hetaOne)./X(:,2)).*X(:,1).*X(:,1)./X(:,2).*
...(1-exp(-z.*X(:,2)))./z./X(:,2).*(1-exp(-ksi.*X(:,2)))./ksi./X(:,2).*mx*my;
heta = [0.0065];
heta0 = [0.004];

rng('default') % for reproducibility

opts = statset('nlinfit');opts.RobustWgtFun ='bisquare';
mdl3= fitnlm(X,theoretical_b,B,heta0,'Options',opts)
hetaInf=mdl3.Coefficients.Estimate;

modelled_b=B(hetaInf,X);

[Comparison,gof]=fit(modelled_b,theoretical_b,'poly1');

Coeffs=table(mx,my,z,ksi,hetaOne,hetaInf)
end
```

Furthermore, this algorithm calculates a and b terms based on Wang's model :

```
function [mx,my,z,ksi,hetaOne,hetaInf,name,heta,Pinteraction,Ptrack,Pcorrect,...
Pcontribution,a,b]=step2(n,lambdap,np,N,Y,Coeffs)
% Parameters V79
mx=Coeffs.mx;
my=Coeffs.my;
z=Coeffs.z;
ksi=Coeffs.ksi;
hetaOne=Coeffs.hetaOne;
hetaInf=Coeffs.hetaInf;
name='V79';

% NHEJ pathway
heta=hetaInf-(hetaInf-hetaOne)./lambdap;
Pinteraction=@(heta,np) (1-exp(-heta.*np))./(heta.*np);
Ptrack=@(ksi,lambdap) (1-exp(-ksi*lambdap))./(ksi*lambdap);
Pcorrect=mx*Pinteraction(heta,np).*Ptrack(ksi,lambdap);
Pcontribution=@(z,lambdap) (1-exp(-z*lambdap))./(z*lambdap);
% Average number of lethal events
Ndeath=my.*N.*Pcontribution(z,lambdap).*(1-Pcorrect);
Sexperimental=exp(-Ndeath);
a=Y.*Pcontribution.*(1-mx*(Ptrack)).*my;
b=0.5*heta.*Y./lambdap.*Y.*Pcontribution.*Ptrack.*mx.*my;

end
```